Deep–Sea Research I 208 (2024) 104303

Contents lists available at ScienceDirect

Deep-Sea Research Part I

journal homepage: www.elsevier.com/locate/dsri

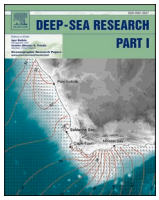

Predicting the distribution of megabenthic communities on deep-water seamounts with cobalt-rich crusts in the Magellan Seamount Chain in the northwestern Pacific ocean

Runxuan Yan [a,b], Chengcheng Shen [b,c,*], Dongsheng Zhang [b,c,d], Zhenggang Li [e], Leyi Fang [b], Chunsheng Wang [a,b,c,d,**]

[a] College of Oceanography, Hohai University, Nanjing, 210098, China
[b] Key Laboratory of Marine Ecosystem Dynamics, Second Institute of Oceanography, Ministry of Natural Resources, Hangzhou, 310012, China
[c] Southern Marine Science and Engineering Guangdong Laboratory (Zhuhai), Zhuhai, 519000, China
[d] School of Oceanography, Shanghai Jiao Tong University, Shanghai, 200240, China
[e] Key Laboratory of Submarine Geosciences, Second Institute of Oceanography, Ministry of Natural Resources, Hangzhou, 310012, China

ARTICLE INFO

Keywords:
Megabenthic communities
Deep-water seamounts
Species distribution models
Vulnerable marine ecosystems

ABSTRACT

Deep-water seamount ecosystems are sensitive to human activities and have a slow recovery rate after being disturbed. Bottom trawling and potential deep-sea mineral extraction could severely damage benthic communities on seamounts and seriously impact deep-sea ecosystems. Inadequate knowledge of the distribution of megabenthos on seamounts or their community structure hinders deep-sea conservation and management. In this study, based on a multidisciplinary dataset generated from recordings taken by human-occupied vehicle (HOV) and remotely operated vehicles (ROVs) along transects and environmental variables, a range of megabenthic morphotaxa were observed on two adjacent deep-water seamounts and predicted using species distribution models (SDMs). Accordingly, based on the predicted distribution of each morphotaxon, five distinct communities were identified through cluster analysis. The results of SDMs showed that environmental variables varyingly impacted the distribution of different morphotaxa, among which the average velocity and eastness direction of near-bottom currents, bathymetric position index (BPI), and backscatter intensity exerted the most significant influence on megabenthic distribution patterns. The distribution of five distinct communities showed a similarity of community composition on the two deep-water seamounts, suggesting a potential connectivity between the two seamounts. The distribution of communities revealed the spatial characteristics of vulnerability of deep-water seamounts at the community level, which could provide a direct basis for marine spatial planning of deep-sea ecosystems.

1. Introduction

Deep-sea ecosystems are progressively imperiled by anthropogenic disturbances, such as waste disposal, oil and gas extraction, deep-sea fisheries, and potential deep-sea mineral extraction (Glover and Smith, 2003). Bottom trawl fisheries harvest target species and remove most of the benthic fauna, alter community composition and food web architecture, and change the seabed environment encompassing modifications to the physical attributes of surface sediments as well as the discharge of chemical contaminants within these sediment layers (Clark et al., 2016; Handley et al., 2014; Mestre et al., 2017; O'Neill et al., 2013). Compared with bottom trawling, the impacts of mining on deep-sea ecosystems are more complex and difficult to predict (Jones et al., 2018; Van Der Grient and Drazen, 2021), which comprise removal of fauna inhabiting mineral deposits, habitat destruction and formation of sediment plumes (Gollner et al., 2017; Miller et al., 2018). Sediment plumes may disperse more than 100 km by variable ocean currents and smother benthic filter feeders (Boschen et al., 2013; Muñoz-Royo et al.,

* Corresponding author. Key Laboratory of Marine Ecosystem Dynamics, Second Institute of Oceanography, Ministry of Natural Resources, Hangzhou, 310012, China.
** Corresponding author. Key Laboratory of Marine Ecosystem Dynamics, Second Institute of Oceanography, Ministry of Natural Resources, Hangzhou, 310012, China.
E-mail addresses: shencc@sio.org.cn (C. Shen), wangsio@sio.org.cn (C. Wang).

https://doi.org/10.1016/j.dsr.2024.104303
Received 23 November 2023; Received in revised form 11 April 2024; Accepted 20 April 2024
Available online 21 April 2024

2021; Pinheiro et al., 2021). To prevent severe impacts of human activities on the deep sea, vulnerable marine ecosystems (VMEs), which are easily disturbed and slow to restore, are identified and protected from bottom fishing activity (Ardron et al., 2014; van Denderen et al., 2022). The conservation of these vulnerable ecosystems is also a desired outcome for environmental management to prevent serious harm to deep-sea ecosystems caused by mining activities (Tunnicliffe et al., 2020). Seamounts serve as habitats for many VME indicator species that are adopted to signal the occurrence of VMEs (Watling and Auster, 2017). Cobalt-rich crusts, as important marine mineral resources, often occur on the surfaces of seamounts (Du et al., 2017). To preserve seamount biodiversity and guide the environmental management of seamounts, studies on the structure and distribution of megabenthic communities on deep-sea seamounts are urgently needed.

Seamounts provide diverse habitats with abundant species and distinct benthic communities (Bo et al., 2020; Clark et al., 2010; Leitner et al., 2021; Yesson et al., 2011). Because seamounts often span a wide range of depths, there are vertical differences in environmental variables, especially depth-related variables such as temperature, dissolved oxygen, aragonite saturation, and particulate organic carbon (POC) flux (Perez et al., 2018). These environmental variables control the vertical distribution of species (Goode et al., 2021) and cause significant species turnover with depth on seamounts (Bridges et al., 2022; Victorero et al., 2018). Rugged and extensively heterogeneous terrains are features of seamounts, inducing intricate hydrodynamic patterns and uneven sediment deposition patterns (Morgan et al., 2015; Tapia-Guerra et al., 2021). These geomorphic attributes give rise to a spectrum of microhabitats, contributing to diverse biological assemblages that thrive in response to distinct settlement conditions (Morgan et al., 2015). The heterogeneous habitats and variable biological communities on seamounts indicate that the spatial distribution of seamount biota cannot be generalized using simple patterns (Clark et al., 2012; O'Hara et al., 2010). The present understanding of seamount ecosystems comes from a minute fraction of seamounts globally (approximately 300 seamounts) subject to biological investigations (Kvile et al., 2014; Xu, 2021). The distribution of seamount fauna remains confined to several case studies, with limited instances focusing on deep-water seamounts (Bridges et al., 2021; Schlacher et al., 2010).

Using species distribution models (SDMs, also known as habitat suitability models or environmental niche models), it is possible to infer the distribution of species across the entire seamount or even multiple seamounts from limited seamount species records (González-Irusta et al., 2015). The reliability of SDMs in deep-sea environments has significantly increased due to enhancements in data quality achieved through the utilization of multibeam echosounder surveys and video surveys to collect high-resolution species data, as well as the development of robust models for presence-only data (Vierod et al., 2014). Constructing SDMs of VME indicator species is a common approach to locate VMEs (Burgos et al., 2020). Among VME indicator species, habitat-forming organisms such as corals and sponges create complex biogenic structures, upholding high biodiversity and enhancing ecosystem functioning (De La Torriente et al., 2020; Xu, 2021). Consequently, habitat-forming organisms garner substantial attention (Anderson et al., 2022; Gonzalez-Mirelis, 2021), and their distribution serves as a crucial reference for fisheries management (Georgian et al., 2019) and marine protected area planning (Graves et al., 2023). Nevertheless, due to limited knowledge of deep-sea ecosystems, the ecological role of many organisms remains poorly understood, possibly introducing biases in assessing the capacity to indicate VMEs of certain species. Furthermore, ecosystems are not exclusively composed of the indicator species; protecting some species in a seamount does not necessarily protect the integrity of the seamount communities, possibly making little sense for the protection of seamount ecosystems (Watling and Auster, 2021). It is imperative to include benthic taxa beyond habitat-forming species in observations and analyses, which can help to enrich our understanding of the vulnerability of deep-water ecosystems. Furthermore, utilizing SDMs to gain insights into the distribution of all biological groups observed within a region is an effective approach (Uhlenkott et al., 2022).

Taking the Caiwei and Weijia seamounts in the northwestern Pacific Ocean as examples, the distribution of a range of benthic megafaunal morphotaxa observed in the study area was predicted using SDMs, and their community structure was revealed using cluster analysis. Thus, the distribution of distinct megabenthic communities in these deep-water seamounts was mapped. The findings of this investigation hold significant potential for informing and advancing strategies pertaining to the conservation and effective management of VMEs of deep-sea seamounts at the community level.

2. Methods

2.1. Study area

The Magellan Seamount Chain is in the northwestern Pacific Ocean and is characterized by ancient oceanic crust and an oligotrophic environment (Hamilton, 2003; Morel et al., 2010). The Caiwei seamount (along with the Caiqi seamount in the southwest) and Weijia seamount (along with the Weixie seamount in the southwest) are distributed from north to south in the Magellan Seamount Chain (COMRA Office, 2018), approximately 350 km apart (Fig. 1). They are typical guyots that have a flat, platform-like top and steep slopes (Table 1). Strong bottom currents are primarily concentrated along the summit margins and ridge branches, with a rapid reduction in bottom flow velocity observed in the summit center and steep cliff regions (Zhao et al., 2020a). Geological surveys indicate that these two seamounts are rich in cobalt-rich crusts and may be concentrated within the depth range of 2000–2500 m at the Caiwei Seamount and 1500–2500 m at the Weijia Seamount (Zhao et al., 2020a, 2020b).

To date, benthic fauna research conducted near the Caiwei and Weijia seamounts has encompassed several new species discoveries (Dong et al., 2019; Shen et al., 2021a; Xu et al., 2017), a comparison of population structure (Na et al., 2021), a geomorphological classification of the Caiwei Seamount (Fan et al., 2022), and a quantitative analysis of the megafaunal community on the Weijia Seamount (Shen et al., 2021b).

2.2. Video data and environmental data

2.2.1. Video data and processing

The video data of the Caiwei seamount were collected from cruises DY31/III in 2013 and DY35/I in 2014 onboard R/V Xiangyanghong 09. The video data of the Weijia seamount were collected from cruises DY37/I in 2016 onboard R/V Xiangyanghong 09, DY41/B in 2017 and DY51/I in 2018 onboard R/V Haiyangdizhi 6, and DY61 in 2020 onboard R/V Dayangyihao. Video materials of Caiwei Seamounts were collected by human-occupied vehicle (HOV) Jiaolong over 10 dives, and video materials of Weijia Seamounts were collected by HOV Jiaolong, remotely operated vehicle (ROV) Hailong III and ROV Haima over 17 dives (Fig. 1; Table 2). Video data with poor quality (obstructed, too dark, blurred, etc.) were excluded to enhance data quality. The reserved video materials, covering 22.9 km of Caiwei Seamounts and covering 29.3 km of Weijia Seamounts, were regarded as effective data used to identify benthic megafauna. These videos were divided into 522 samples, and each sample was 100 m long, as conducted in relevant studies (Victorero et al., 2018; Shen et al., 2021b).

All megafauna were identified at the lowest possible taxonomic level (see Supplementary Table 1). Voucher specimens, used for taxonomic determinations, were collected by HOV or ROV and deposited in the Repository of the Second Institute of Oceanography (RSIO), Hangzhou, China. Organisms resembling those collected and identified specimens were grouped into the same morphotaxon category. In cases where specimens were unobtainable, we referred to previously published video analyses for megafaunal identification from video data (Morgan et al.,

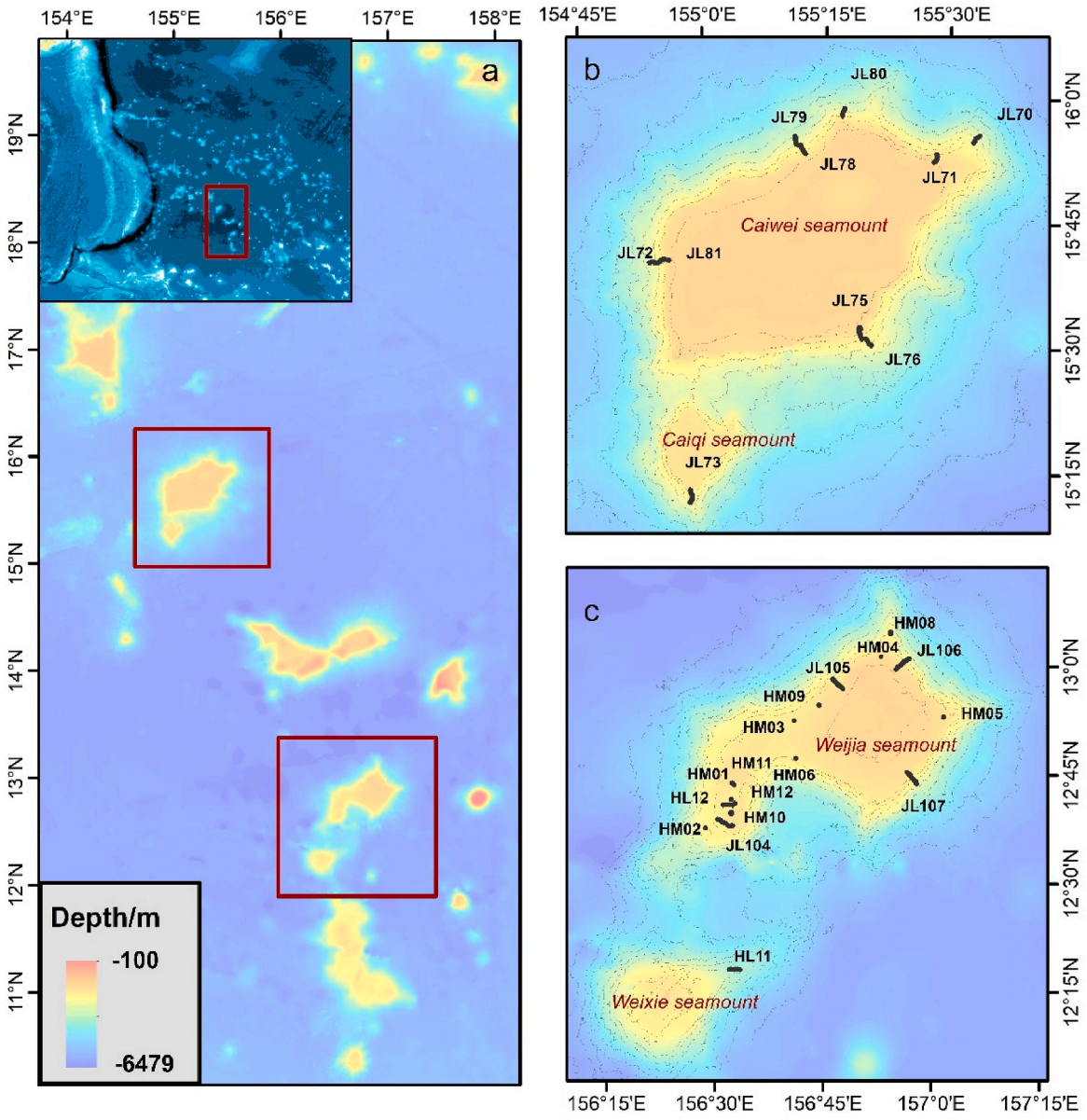

Fig. 1. Map of the study area in the northwestern Pacific (a). Map of the Caiwei seamount along with the Caiqi seamount in the southwest showing the location of human-occupied vehicle (HOV) Jiaolong (JL70–73, JL75–76, JL78–81) tracks (b). Map of the Weijia seamount along with the Weixie seamount in the southwest showing the location of the HOV Jiaolong (HL104–107) and remotely operated vehicle (ROV) Haima (HM01–12) and Hailong III (HL11–12) tracks (c).

Table 1
Shape characteristics of the seamounts. To avoid ambiguity, unless otherwise specified, the plural word Caiwei seamounts refers to the two seamounts Caiwei and Caiqi, and the plural word Weijia seamounts refers to the two seamounts Weijia and Weixie in the article.

Seamounts	Caiwei	Caiqi	Weijia	Weixie
Name in GEBCO	Pallada	/	Ita Mai Tai	Gelendzhik
Top platform depth (m)	1450	1800	1600	1500
Minimum depth (m)	1230	1629	1405	1299
Piedmont depth (m)	4830	5100	6120	6030
Total relief (m)	3600	3471	4715	4731
Length (km) × Width (km)	110 × 95	80 × 54	100 × 75	80 × 45

2015; Schlacher et al., 2014; Shen et al., 2021b). Additionally, taxonomists specialized in specific groups reviewed video segments and digital still images of the organisms in question. When identification proved challenging, taxa were identified to the lowest taxonomic unit possible and categorized into distinct morphotaxa based on characteristics such as shape, color, attachment methods, and other observable traits. Organisms that could not be clearly identified, even at the morphotype level, were categorized as unclear fauna and excluded from analysis. Due to the lack of close-up images for most demersal fishes or shrimps, fishes or shrimps were counted as a single morphotype. Given the limited predictive accuracy associated with infrequently occurring species, to retain as many morphotaxa as possible, we, following the categorization principles outlined by Shen et al. (2021b), undertook additional consolidation of several morphotaxa that exhibited morphological similarities, taxonomic affinity, and highly congruent habitat preferences. In addition, the taxonomy was updated according to the check-list of the World Register of Marine Species (WoRMS: http://www.marinespecies.org/).

In a previous study by Shen et al. (2021b), the analysis encompassed the processing of data from 15 dives conducted on the Weijia Seamount. In the present investigation, we augmented this dataset by incorporating

Table 2
Information on the HOV and ROV dives used in this study. Effective distance refers to the distance covered by the video after discarding poor-quality video segments. Geographical positions are shown, with the beginning and end points of each dive (beginning longitude–end longitude; beginning latitude–end latitude), while for some short dives, only the beginning point is used to represent the geographical position of the dive sites.

Seamount	Curise/Leg	Dives	Data (dd/mm/ww)	Effective distance/km	Longitude/°E	Latitude/°N	Depth/m
Caiwei	DY31/III	JL70	September 04, 2013	1.9	155.557–155.544	15.930–15.915	2710–1984
Caiwei	DY31/III	JL71	September 06, 2013	2.1	155.471–155.465	15.893–15.877	1938–1421
Caiwei	DY31/III	JL72	September 07, 2013	2.3	154.895–154.915	15.676–15.678	2770–2167
Caiqi	DY31/III	JL73	September 09, 2013	3.1	154.976–154.977	15.197–15.222	2409–1819
Caiwei	DY35/I	JL75	July 16, 2014	4	155.320–155.315	15.523–15.544	2385–1532
Caiwei	DY35/I	JL76	July 17, 2014	2.1	155.340–155.328	15.511–15.524	2736–2385
Caiwei	DY35/I	JL78	July 21, 2014	2.1	155.198–155.208	15.910–15.894	2385–1552
Caiwei	DY35/I	JL79	July 22, 2014	2	155.186–155.193	15.929–15.911	3134–2473
Caiwei	DY35/I	JL80	July 23, 2014	1.8	155.286–155.282	15.985–15.969	3335–2414
Caiwei	DY35/I	JL81	July 25, 2014	1.5	154.916–154.934	15.680–15.681	2082–1533
Weijia	DY37/I	JL104	April 28, 2016	4.7	156.510–156.541	12.650–12.634	1960–1763
Weijia	DY37/I	JL105	April 30, 2016	3.9	156.770–156.797	12.970–12.949	2269–1542
Weijia	DY37/I	JL106	May 01, 2016	4.4	156.950–156.919	13.020–12.995	2658–1533
Weijia	DY37/I	JL107	May 04, 2016	4.2	156.970–156.944	12.730–12.757	2763–1692
Weijia	DY41/B	HM01	September 27, 2017	0.5	156.538	12.695	1686
Weijia	DY41/B	HM02	September 22, 2017	0.8	156.479	12.629	2017
Weijia	DY41/B	HM03	September 17, 2017	0.2	156.683	12.877	1878
Weijia	DY41/B	HM04	September 18, 2017	0.6	156.885	13.024	1579
Weijia	DY41/B	HM05	September 19, 2017	0.4	157.029	12.885	1649
Weijia	DY41/B	HM06	September 21, 2017	0.4	156.688	12.79	1938
Weijia	DY51/I	HM08	August 29, 2018	1.4	156.906	13.077	2341
Weijia	DY51/I	HM09	August 28, 2018	0.4	156.742	12.911	1740
Weijia	DY51/I	HM10	August 30, 2018	1	156.539	12.662	1736
Weijia	DY51/I	HM11	August 30, 2018	0.9	156.540	12.732	1894
Weijia	DY51/I	HM12	September 20, 2018	0.6	156.546	12.684	1699
Weixie	DY61	HL11	October 12, 2020	2.7	156.559–56.534	12.302–12.303	2477–2377
Weijia	DY61	HL12	October 13, 2020	2.2	156.520–156.541	12.681–12.682	1865–1705

two additional dives on the Weijia Seamounts and 17 dives on the Caiwei Seamounts.

2.2.2. Environmental data and processing

Multibeam bathymetry and backscatter data of the Caiwei and Weijia Seamounts were collected using the ship's hull-mounted Kongsberg EM122 echo sounder and processed using CARIS HIPS and SIPS 9.1 (Shen et al., 2021b; Yang et al., 2020a). Terrain analysis was performed using ArcGIS 10.8 with a raster resolution of 100 m (Table 3). Terrain parameters, including slope, roughness, aspect, curvature and bathymetric position index (BPI), were derived from bathymetric data (Li et al., 2021). The aspect was split into two components: Eastness, obtained as sin (aspect); and northness, obtained as cos (aspect) (Rodríguez-Basalo et al., 2021; Wilson et al., 2007). The seamount topography was divided into five categories by iterative self-organizing data analysis (ISODATA) on the basis of the BPI and slope parameters: (1) low depression area, (2) moderately depressed area, (3) flat area, (4) moderately elevated area, and (5) highly elevated area (Shen et al., 2021b; Yang et al., 2020b).

The parameters of the velocity and direction of the near-bottom current with a resolution of 3 km were extracted from a numerical simulation of the Coastal and Regional Ocean Community (CROCO) model in the northwestern Pacific Ocean from 2011 to 2015 (Jiang et al., 2021). In this model, the horizontal resolution is 1/36°, and it is vertically divided into 48 layers. Five-year daily average values of the near-bottom current direction and velocity from 2011 to 2015 were calculated, and kriging interpolation was used to increase the resolution of the rasters to 100 m (Table 3). The parameter of the current direction was split into two components in a similar manner as the parameter of aspect.

2.3. Species distribution model

Ensemble models are thought to provide robust forecasts of species distribution using several modeling methods in which a measure of central tendency can be quantified (Araujo and New, 2007; Deka and Morshed, 2018). Assembling a group of models that employ fundamentally distinct approaches to address the same problem provides a practical means to reduce reliance on a single model type or structural assumption (Robert et al., 2016). This approach enhances the capacity

Table 3
Descriptions of environmental variables.

Type	Variable	Description	Produced in:
Terrain variables	Depth (m)	Bathymetric surface representing depth	Arcgis 10.8
	Slope (°)	Rate of change in depth	Arcgis 10.8
	Aspect northness	Direction of slope: orientation on north–south scale	Arcgis 10.8
	Aspect eastness	Direction of slope: orientation on east–west scale	Arcgis 10.8
	Curvature	Second spatial derivative of the seabed terrain, describes the surface fluctuation	Arcgis 10.8, 3 × 3 neighborhood
	Bathymetric position index (BPI)	Describes the surface fluctuation such as crest (positive value) and trough (negative value)	Arcgis 10.8, 3 × 3 neighborhood
	Topographic type	Five categories of seamount topography	Arcgis 10.8
	Backscatter (dB)	Measure of reflectivity of seabed, corresponding to substrate type	CARIS HIPS and SIPS 9.1
	Roughness	Describes the surface roughness	Arcgis 10.8
Current variables	Velocity (m/s)	Near-bottom current speed	CROCO model
	Current northness	Direction of near-bottom current: orientation on north–south scale	CROCO model
	Current eastness	Direction of near-bottom current: orientation on east–west scale	CROCO model

to robustly describe the predicted spatial variations and associated uncertainties (Robert et al., 2016).

Morphotaxa with an occurrence frequency of more than 10 were selected as objects for species distribution prediction. The distribution of these morphotaxa was modeled based on occurrence records and environmental variables using the R package *Biomod2* 4.2–3, an ensemble platform for species distribution modeling. Seven algorithms were used for modeling, including the generalized additive model (GAM), gradient boosted machine learning (GBM), classification tree analysis (CTA), random forest classifier (RF), flexible discriminant analysis (FDA), multiple adaptive regression splines (MARS), and maximum entropy model (MAXENT). All the algorithms featured the *biomod2* default model settings.

In the process of modeling, 1000 pseudo-absence points were randomly selected instead of real absences, and this process was repeated 3 times (Barbet-Massin et al., 2012). Seventy percent of the coupled occurrences and pseudo-absence data were randomly selected as the training dataset, and the remaining 30% were used as the testing dataset. The division of data was also repeated 3 times. A total of 63 different SDMs were established for each morphotaxon. The scope of modeling was limited to depths of 1400–3500 m on the Caiwei seamounts and 1500–3500 m on the Weijia seamounts at a 100 m × 100 m resolution, covering an area of 6053 km^2. The depth range was selected, accounting for the depth of the observation, to enhance the accuracy of the model forecasts. The incorporation of correlated environmental variables can potentially impede both model performance and interpretability. In practice, it is often necessary to omit highly correlated environmental variables from the modeling process to mitigate issues related to collinearity within statistical models (Dormann et al., 2013). Therefore, measures of variance inflation factors (VIF) and Spearman correlation were performed on all environmental variables (Naimi et al., 2014; Zhao et al., 2021). Biological observation in this study area was limited to a relatively narrow range of depths within a bathyal zone (ranging from 1421 m to 3335 m), which implied less variation in physical or chemical conditions compared to those covering the water layers from the euphotic zone to the twilight zone. Moreover, a previous study on the Weijia Seamount showed that the statistical significance of depth correlated with megabenthic communities was mainly contributed by the spatial heterogeneity of terrain-related variables (Shen et al., 2021b). This was consistent with the findings of a case study on the megabenthic community structure of cobalt-rich crusts on the Necker Ridge with comparable sampling depths of 1400–2000 m (Morgan et al., 2015). Accordingly, the variable of depth was not considered when constructing the models.

The area under the receiver operating characteristic curve (AUC) was calculated as an alternative measure of model evaluation (Gama et al., 2017). Prediction accuracy is categorized as follows: AUC values below 0.5 are considered similar to random, those between 0.5 and 0.7 are considered poor, values in the range of 0.7–0.9 are considered fair, and AUC values exceeding 0.9 are deemed excellent (Gama et al., 2017; Zhao et al., 2021). The ensemble model of each morphotaxon was constructed using a weighted approach based on AUC scores of five top-scoring SDMs. The coefficient of variation (CV, the ratio of standard deviation to mean value) over the selected model outputs was calculated as a measure of model uncertainty (Anderson et al., 2016; Ramiro-Sánchez et al., 2019). A higher CV indicates greater uncertainty in predicted species occurrence.

To obtain the most important predictors for the distribution, *biomod2* calculates the variable importance by correlating the fitted values of the full models with the ones from the model in which the values of the predictor have been randomly permuted (Gama et al., 2017). The value range of variable importance falls between 0 and 1, where a higher value indicates a greater impact of the variable on the model.

Two rasters were output from the ensemble model of each morphotaxon, including a habitat suitability score raster and a binary presence-absence raster. The former represents the relative predicted suitability, which does not represent the actual probability of occurrence due to the lack of true absence data and unknown efficiency of the sampling gear (Georgian et al., 2019). To distinguish it from the "probability of occurrence", we made the relative predicted suitability scores range from 0 to 1000 than from 0 to 1. The latter shows the areas where morphotaxa are most likely to be distributed. The threshold that maximizes the AUC scores was used to transform the output of SDMs into a binary presence-absence raster.

2.4. Statistical analyses

Spearman's correlation matrix was calculated using the R package *vegan* 2.6–4, and the VIF among the environmental variables was calculated using the R package *usdm* 2.6–4.

The importance of environmental variables for the distribution of morphotaxa was analyzed using complete linkage clustering based on Pearson correlation distances, and the results were visualized with the R package *pheatmap* 1.0.12.

Using the R package *vegan* 2.6–4, K-means cluster analysis for predicted habitat suitability scores of morphotaxa was performed to distinguish the megabenthic communities (Uhlenkott et al., 2022). Accordingly, five clusters were determined based on an elbowplot (Swanborn et al., 2023) (Supplementary Fig. 1) and a previous study on the megabenthic communities on the Weijia Seamount (Shen et al., 2021b). The visualization of community distributions was achieved using the R package *terra* 1.7–29.

3. Results

3.1. Environmental conditions

The descriptive statistics of environmental variables within this locale are shown in Fig. 2. The northness of the seamount aspect exhibited no statistically significant difference between the two seamounts ($p > 0.05$). The backscatter intensity, slope, eastness of the seamount aspect, and eastness and northness of the near-bottom current direction on the Caiwei Seamount demonstrated significantly higher values than those on the Weijia Seamount ($p < 0.01$). The BPI, curvature, depth and average velocity of near-bottom currents exhibited significantly lower values on the Caiwei Seamounts than those on the Weijia Seamounts ($p < 0.01$).

Spearman correlation analysis was performed for each of the two environmental variables (Supplementary Fig. 2). Slope and roughness, as well as topographic type and BPI, were two pairs of variables that were highly correlated. To prevent a strong correlation between variables affecting the stability of SDMs, the variables of slope and topography type were excluded when constructing the models.

3.2. Composition of benthic megafauna

A total of 94 morphotaxa were classified based on the 6436 megabenthic individuals observed and counted on the Caiwei and Weijia Seamounts. The megafauna on the two seamounts mostly comprised five phyla: Porifera, Cnidaria, Echinodermata, Arthropoda, and Chordata. Among the total individuals, those living on the Caiwei Seamount accounted for 43.8%. Among the total morphotaxa, 70 and 66 morphotaxa were observed on the Caiwei and Weijia Seamounts, respectively; 47 morphotaxa were common on the two seamounts; and 15 morphotaxa were observed only once.

A total of 32 morphotaxa had frequencies of occurrence of more than 10, making them suitable for distributional prediction (Fig. 3). Shrimps appeared with the highest frequency, appearing in 32.8% of the samples. The fishes and crinoid Pentametrocrinidae were the most frequently occurring morphotaxa on the Caiwei and Weijia seamounts, respectively, and their frequency of occurrence varied greatly between the two seamounts. Keratoisididae (unbranched) spp. indet. was the

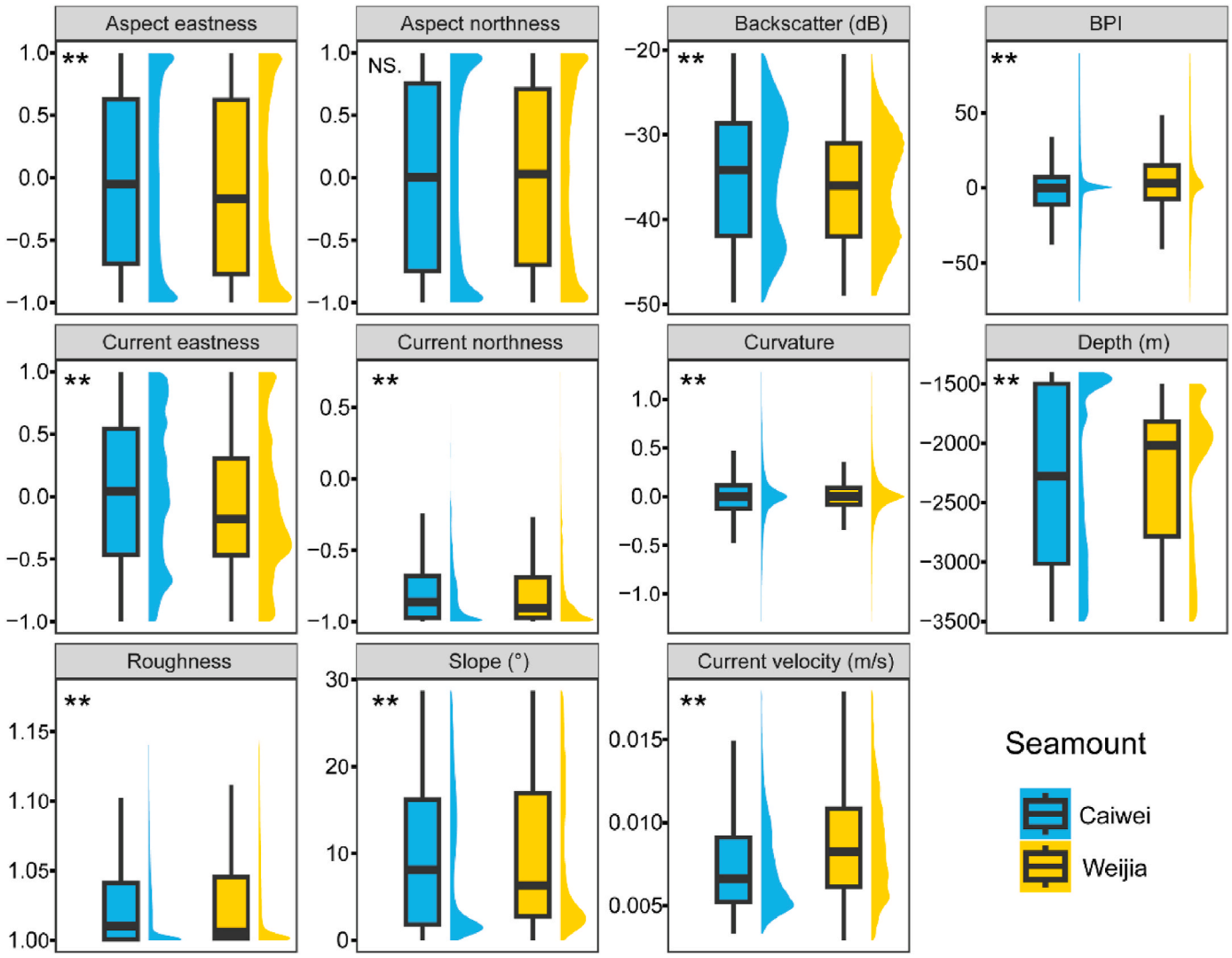

Fig. 2. Half violin box plots of environmental variables on the Caiwei and Weijia seamounts. The Mann−Whitney *U* test was used to assess the differences in environmental variables between the two seamounts. BPI refers to bathymetric position index. ** refers to $p < 0.01$, NS. refers to $p > 0.05$.

most frequent coral on the two seamounts. Holothurian *Enypniastes eximia* and crinoid *Guillecrinus* spp. indet. were found only on the Caiwei seamount and Weijia seamount, respectively, and *Poliopogon* spp. indet. was the most frequent sponge.

3.3. Model performance and uncertainty

The AUC scores of the SDMs used to construct the ensemble models all exceeded 0.7, indicating the reliability of the model performance (Supplementary Fig. 3). Among the seven modeling algorithms considered, the GAM exhibited the most robust stability. The AUC scores of GBM, MANNET and RF demonstrated greater variability. The distribution results of the ensemble model output for each morphotaxon were shown in Supplementary Figs. 4 and 5.

To inform the model uncertainty, the CV for each predicted morphotaxon was calculated with the spatial distribution shown in Supplementary Figs. 6 and 7 and the descriptive statistics presented in Fig. 4. *Metallogorgia.* spp. indet., *Platylistrum subviridum* sp. inc. and *Benthodytes* spp. indet. were the top three morphotaxa with the greatest uncertainty among the predicted 32 morphotaxa, while shrimps, Keratoisididae (unbranched) spp. indet. and *Caulophacus* spp. indet. were the top three morphotaxa with the least uncertainty (Fig. 4). Compared to the observed relative frequency of occurrence, it was implied that morphotaxa occurring in more samples tended to have lower uncertainty of prediction.

The mean CV of the predicted 32 morphotaxa was calculated to describe the spatial difference of predictive bias. Results showed that the seamount ridges and the southwest of Weijia Seamount were featured with relatively least predictive bias, whereas the summits exhibited the relatively greatest uncertainty (Fig. 5). It may result from the more sampling efforts on the seamount ridges than that on the summits.

3.4. Distribution of benthic megafauna and environmental drivers

Among the nine environmental variables considered in the models, the average velocity and eastness of near-bottom currents, BPI, and backscatter intensity emerged as the four most influential variables, contributing significantly to the distribution of the majority of morphotaxa (Fig. 6). Among the 32 morphotaxa examined, eight were notably affected by the velocity of currents, including crinoid *Thalassometra electrae* sp. inc., holothurian *Peniagone* spp. indet., two ophiuroids, two sponges and two corals. According to the model outputs shown in Supplementary Figs. 4 and 5, the two sponges and two ophiuroids occurred mostly in the southern part of the Weijia Seamount and the northern part of the Weixie Seamount, and the distribution range of black coral (Antipatharia spp. indet.) was much smaller than that of sea

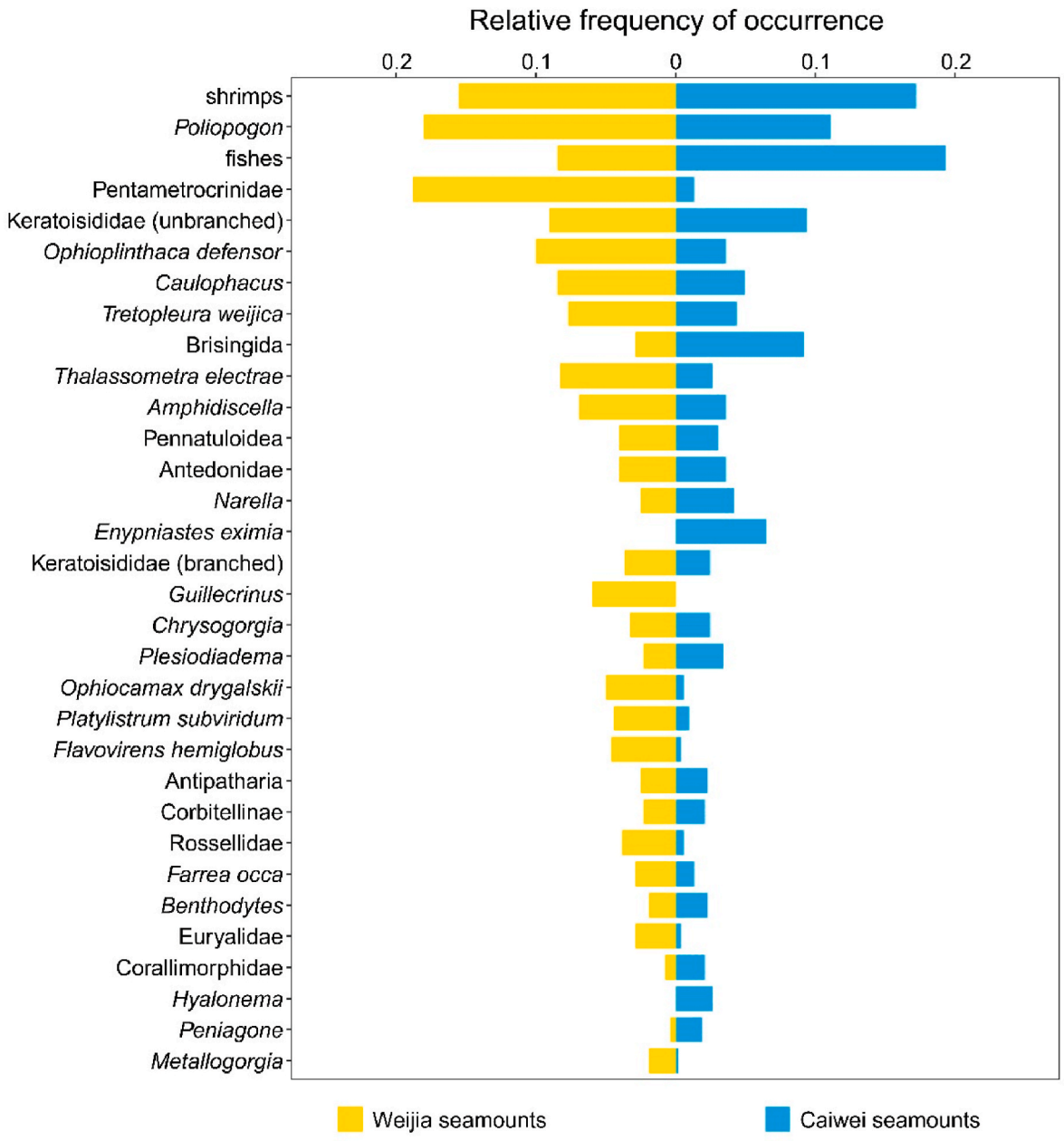

Fig. 3. Relative frequency of occurrence of 32 morphotaxa on the Caiwei and Weijia seamounts. Morphotaxa occurring in more than 10 samples are shown. Morphotaxa are ranked in order of total relative frequency of occurrence.

pens (Pennatuloidea spp. indet.).

Additionally, eight morphotaxa exhibited a shared significant influence of average velocity and direction of near-bottom currents, including fishes, shrimps, the holothurian *Enypniastes eximia*, *Benthodytes* spp. indet., the sea urchin Plesiodiadema spp. indet., crinoid *Guillecrinus* spp. indet., the sponge *Hyalonema* spp. indet., and the coral *Metallogorgia* spp. indet. The first five morphotaxa possessed locomotor ability and were mainly found on the lower flanks (Supplementary Figs. 4 and 5).

Furthermore, seven morphotaxa predominantly responded to variations in backscatter intensity, including filter-feeding organisms such as Brisingida spp. indet., three coral species, two sponge species, and the commensal ophiuroid Euryalidae spp. indet. According to the model outputs, these organisms were mainly distributed on steep slopes (Supplementary Figs. 4 and 5).

The remaining nine morphotaxa exhibited the most significant response to BPI, which encompassed five sponge species, two coral species, and the solitary-growing crinoid Pentametrocrinidae spp. indet., and the crinoid Antedonidae spp. indet., which displayed a preference for clustering on sponges. Most also tended to live on steep slopes (Supplementary Figs. 4 and 5).

3.5. Benthic megafauna community

The benthic megafauna on the Caiwei and Weijia seamounts were divided into five communities by K-means cluster analysis (Figs. 7 and 8). On the Weijia Seamounts, the distribution areas of the communities were similar in size, except for community 5, while on the Caiwei Seamounts, community 1 and community 2 occupied significantly less area than community 3 and community 4. Among the five communities on the Caiwei and Weijia seamounts, community 5 was the largest in area. Furthermore, the environmental conditions among the five communities exhibited significant differences (Fig. 9).

Community 1 surrounded the seamounts and presented a long,

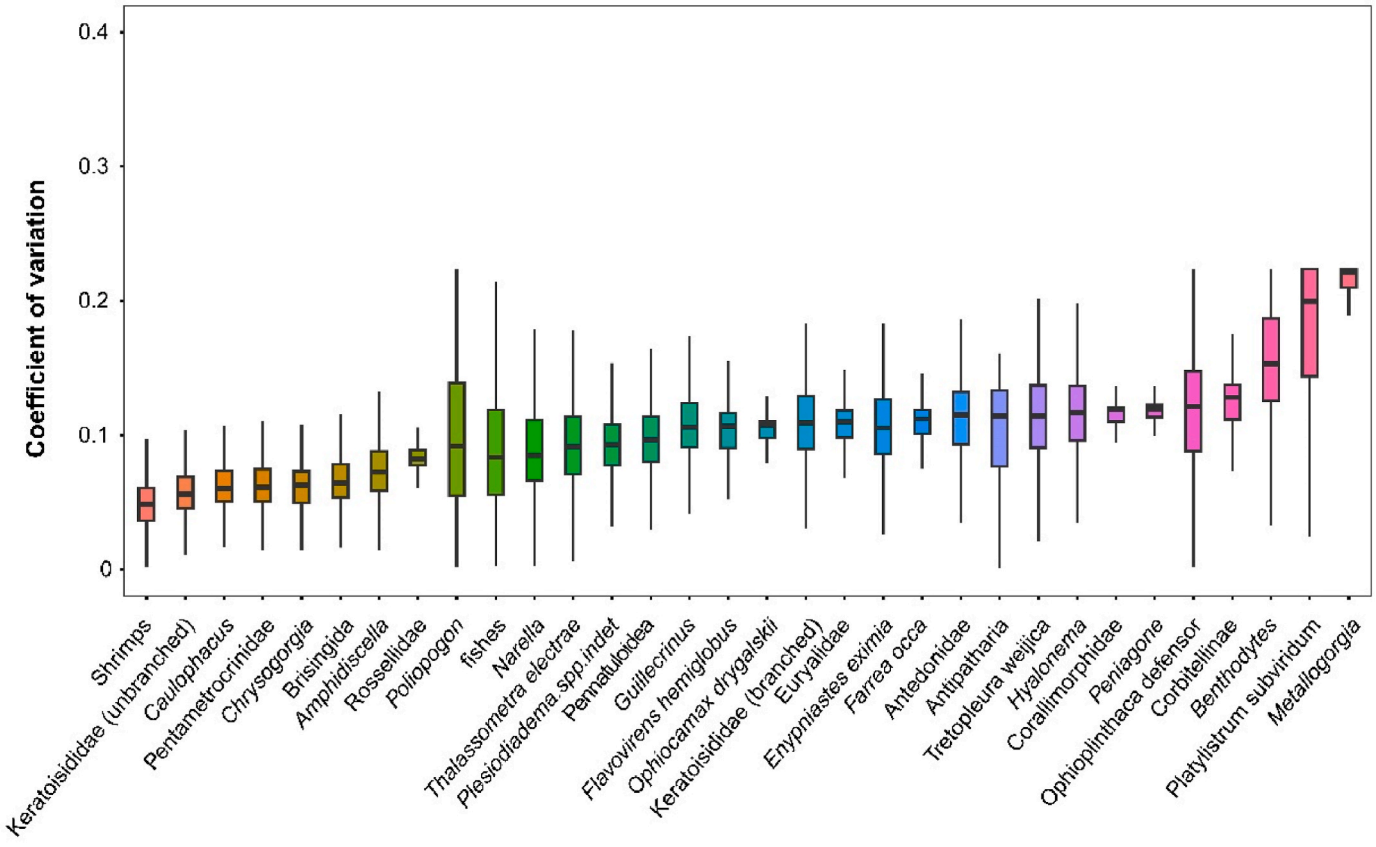

Fig. 4. Coefficient of variation of 32 morphotaxa being modeled on the Caiwei and Weijia seamounts to indicate the uncertainty of each model.

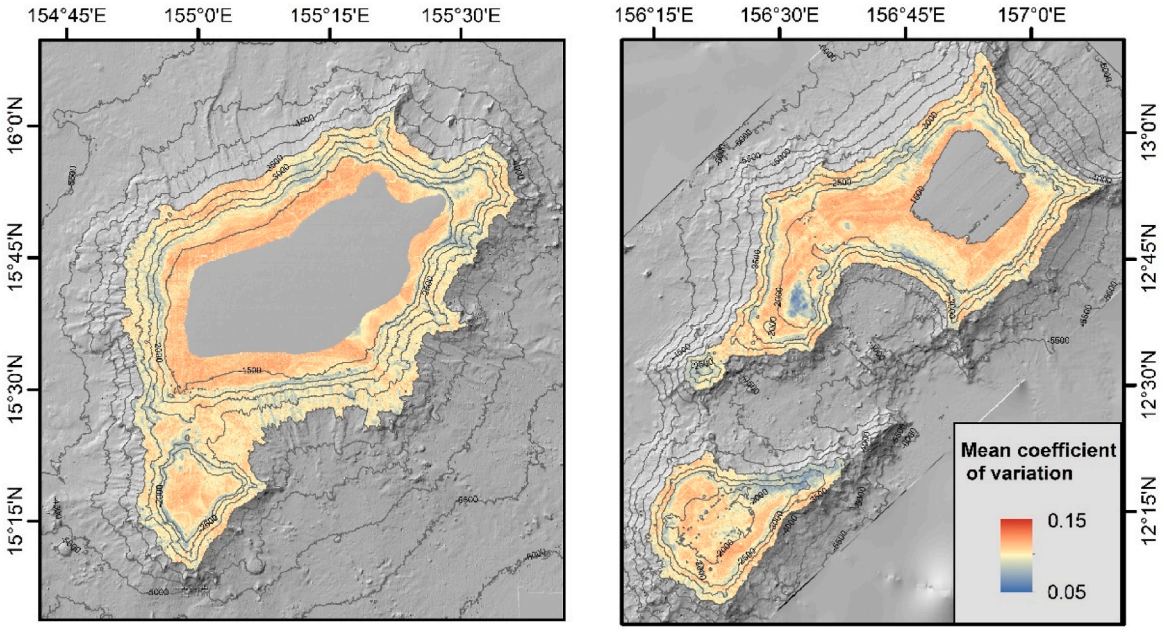

Fig. 5. Spatial distribution of mean coefficient of variation of the predicted 32 morphotaxa on the Caiwei and Weijia seamounts.

narrow "corridor" shape. The most frequently occurring morphotaxa in Community 1 included coral *Chrysogorgia* spp. indet. (47.1%), crinoid Antedonidae spp. indet. (43.8%), sponge *Caulophacus* spp. indet. (40.6%), and *Tretopleura weijica* sp. inc. (36.5%). In Community 1, the proportion of corals and sponges was relatively high; Ophiuroid Euryalidae spp. indet. was typically found attached to corals; ophiuroid *Ophioplinthaca defensor* sp. inc. and crinoid Antedonidae spp. indet. were commonly associated with coral and sponges. Therefore, there were many microhabitats structured by hexactinellid sponges and octocorals present within Community 1. A relatively highest value of both BPI and curvature was shown in the area associated with Community 1 (Fig. 9).

Community 2 was mostly found between the Caiwei Seamount and

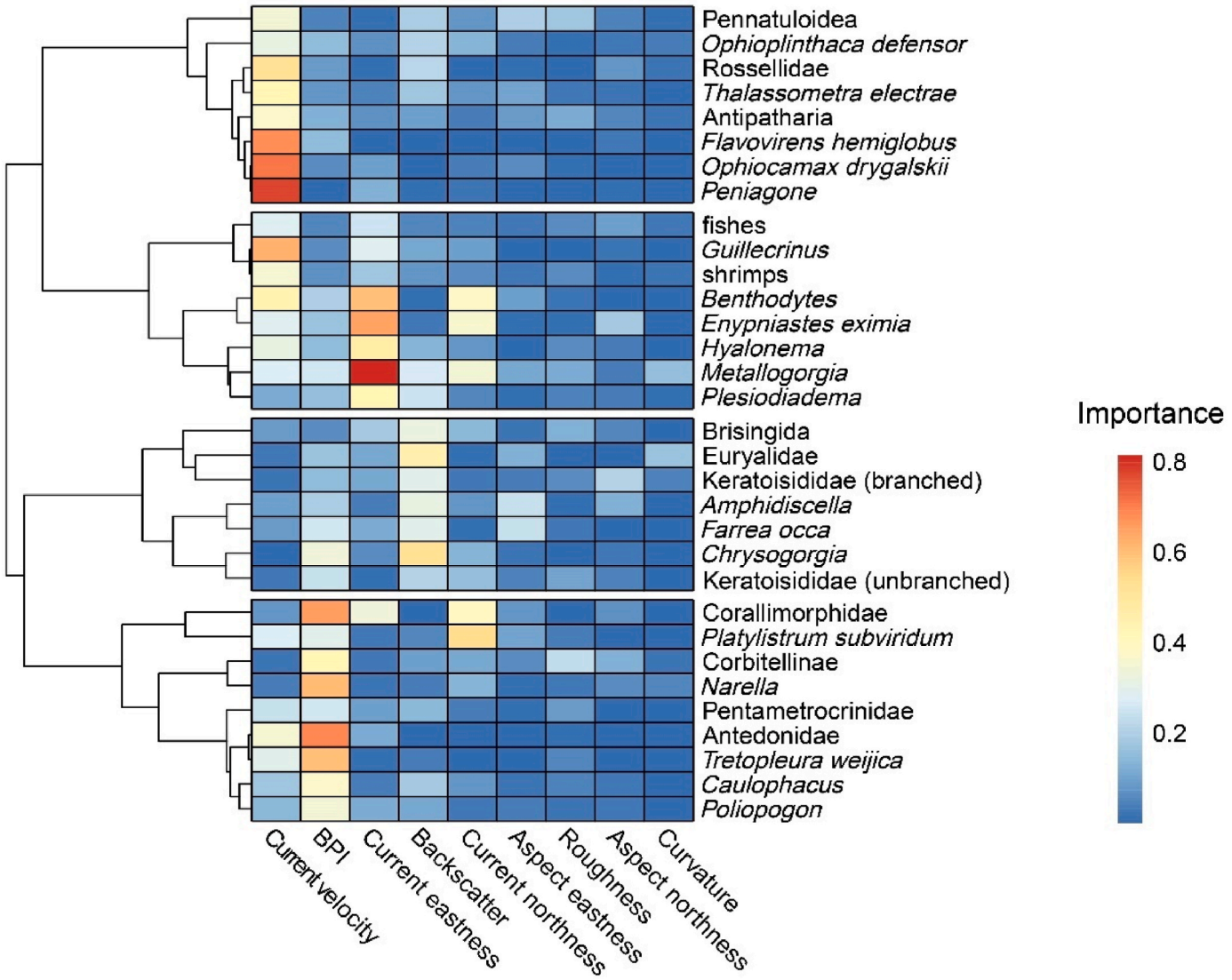

Fig. 6. Importance of environmental variables for the distribution of the 32 morphotaxa on the Caiwei and Weijia seamounts. The importance is output from the ensemble models of each morphotaxon. BPI refers to bathymetric position index.

Caiqi Seamount, in the southwest of the Weijia Seamount, and in the east of the Weixie Seamount. The most common morphotaxa within Community 2 included Rossellidae spp. indet. (44.5%), Pentametrocrinidae spp. indet. (31.0%), and *T. electrae* sp. inc. (29.1%). In Community 2, the occurrence relative frequency of seven organisms was higher than in other communities, including three crinoids, two sponges and two corals. The area corresponding to Community 2 demonstrated the highest velocity of near-bottom currents (Fig. 9).

Community 3 was primarily composed of coral *Chrysogorgia* spp. indet. (47.9%), sponge *Amphidiscella* spp. indet. (25.2%) and coral Keratoisididae spp. (unbranched) indet. (24.4%). This community was mostly distributed in the foothills as well as near Community 1. The *Chrysogorgia* spp. indet. stood out as the morphotaxon in Community 4 with the highest occurrence relative frequency. Their high occurrence frequency in all communities suggested that they were widely distributed on the Caiwei and Weijia seamounts. Community 3 was situated in an area characterized by elevated levels of backscatter and the northness of seamount aspect (Fig. 9).

Community 4 was primarily composed of shrimps (34.0%), fishes (18.5%), and coral *Chrysogeorgia* sp. indet. (15.5%). This community was mostly distributed on the lower flanks of the Caiwei and Weijia seamounts. Three holothurians exhibited a higher occurrence relative frequency within Community 4 compared to other communities. Among them, a shared characteristic was their preference for inhabiting soft substrates. The prevalence of sediments in the geographical region where Community 4 was distributed could account for this phenomenon. The locale of Community 4 was marked by the highest values of roughness and the eastness of currents (Fig. 9).

The occurrence of morphotaxa in Community 5 was extremely rare, implying a low abundance of organisms in the area where Community 5 was located. Community 5 was primarily distributed near the summits, with the most commonly occurring morphotaxa in this area being the sponge Rossellidae spp. indet. (2.9%) and the sea urchin *Plesiodiadema* spp. indet. (1.8%). The geographical attributes relevant to Community 5, including BPI, curvature, and roughness, showed a relatively least variability (Fig. 9).

4. Discussion

4.1. Species distribution and environmental drivers

In the present study, the distribution of 32 morphotaxa of benthic megafauna was mapped across two adjacent deep-water seamounts. The seamount ridges provide suitable habitats for most of the morphotaxa

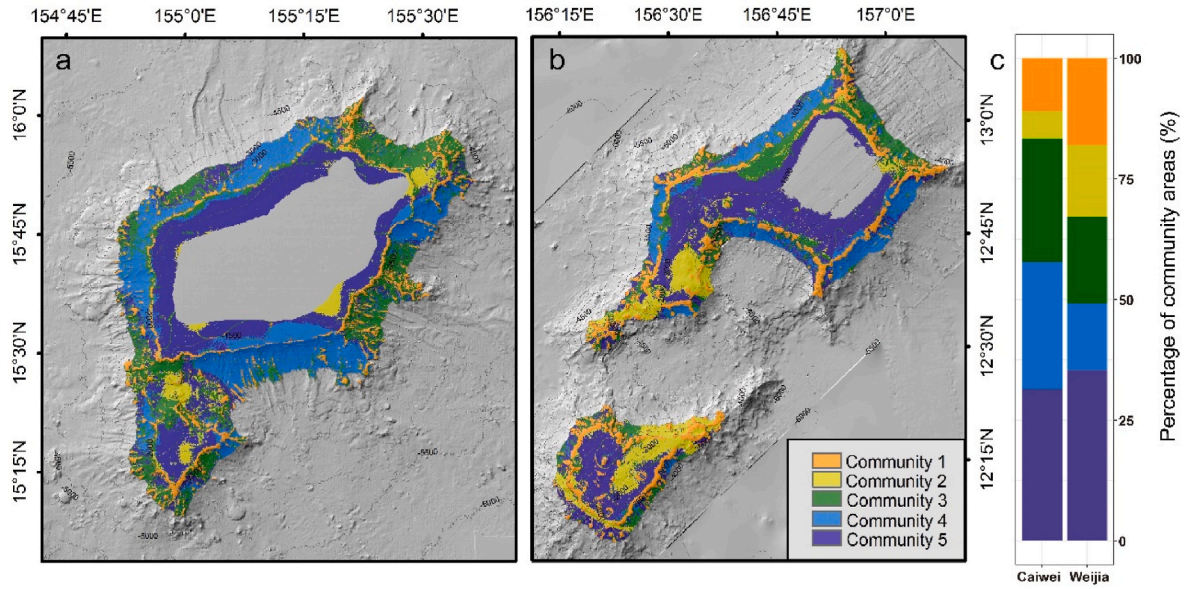

Fig. 7. Distribution of five benthic megafaunal communities (Community 1 to 5) grouped by a K-means cluster analysis on the Caiwei Seamounts (a) and Weijia Seamounts (b), and percentages of megafaunal community areas in each seamount (c). The depth ranges of interest for this study were 1400–3500 m on the Caiwei seamounts and 1500–3500 m on the Weijia seamounts.

observed. These prominent and rugged landforms offer appropriate substrates for larval settlement of cold-water corals and hexactinellid sponges and accelerate local current velocities to enhance habitat quality by increasing food supply (Georgian et al., 2019). Corals and sponges, as habitat-forming species, are highly represented in megabenthic communities and provide food, refuge and breeding grounds for other organisms (Angelini et al., 2011; De La Torriente et al., 2020; Ross et al., 2015). They may coexist within communities as multiple foundation species or participate in one-way nested facilitation cascades, where one foundation species supports the establishment of others (Dijkstra et al., 2021). As a result, the ridges of seamounts exhibit heightened biodiversity.

The Caiwei and Weijia seamounts are located in oligotrophic oceanic regions, with summit depths deeper than 1000 m. Almost all the POC generated through primary productivity has been remineralized before reaching the deep-water seamounts (Henson et al., 2012). Therefore, megabenthic organisms on these seamounts may face food scarcity and rely heavily on those transported by water currents (Bridges et al., 2021; Leduc et al., 2014). The model outputs from this study conclusively demonstrated that environmental variables associated with water currents are the primary factors significantly influencing the distribution of most species. The holothurians were most profoundly affected by these variables. *E. eximia* and *Peniagone* spp. indet. are active swimmers, yet their swimming capabilities are limited, causing them to be less adept at coping with stronger water currents (Kremenetskaia et al., 2021; Robison, 1992). In contrast, *Benthodytes* spp. indet. exhibits sedentary behavior without being disturbed and often crawls on the sediment surface (Bisol et al., 1984). To prevent themselves and the sediments from being carried away by currents, they tend to prefer habitats with lower flow velocities. Filter-feeding or suspension-feeding organisms rely on stronger water currents to ensure an abundant food supply. Their habitats, characterized by intricate and rugged topography, often serve to augment flow velocities at small scales (Victorero et al., 2018). Consequently, at 100-m scales, their distribution is more significantly influenced by topographical variables (Goode et al., 2021).

BPI serves as a measure of the relative elevation of the central cell when compared to the surrounding cells and represents both exposure to currents and the nature of the seabed (Miyamoto et al., 2017; Wilson et al., 2007). Therefore, BPI stands out as the variable in this study that best encapsulates the steepness and elevation characteristics of the environmental background. Numerous studies have consistently revealed the profound impact of BPI on deep-sea species distributions (De La Torriente et al., 2019; Rodríguez-Basalo et al., 2021; Taranto et al., 2023), albeit with some exceptions (Burgos et al., 2020). Most of this variation can be attributed to the specific species and spatial scales under consideration. Different species exhibit distinct preferences for BPI, with many favoring horizontal or vertical surfaces on seamounts (Victorero et al., 2018). Nevertheless, certain widely distributed morphotaxa, such as fishes, shrimps, and coral *Chrysogorgia* spp. indet., display a lower sensitivity to topographical features. Spatial scales also serve a function, as larger scales tend to exhibit less pronounced variations in BPI, partly due to reduced resolution (Miyamoto et al., 2017) and partly because of the increased influence of other environmental variables (Anderson et al., 2022). In addition, the other terrain-related variables, including aspect, curvature, and roughness, have a limited contribution to species predictions in the model (Hefley et al., 2013; Kearney and Porter, 2009; Naimi et al., 2014), suggesting a notably weaker influence on species distribution compared to BPI.

Backscatter intensity serves as an indicator of substrate characteristics, including roughness and hardness, and it exhibits clear correlations with grain size (De La Torriente et al., 2019). The nature of benthic habitats is highly contingent upon the substrate type, with backscatter intensity being employed for habitat identification (De Falco et al., 2010). The presence of benthic organisms can also influence backscatter intensity. Evidently, backscatter intensity is not an independent environmental variable, and its values are subject to the influence of multiple factors. When considering its utilization as a factor in predicting species distribution, it is crucial to account for additional relevant information (De Falco et al., 2010; Holmes et al., 2008). In the deep-sea environment, due to the sparse distribution of benthic organisms, the formation of biological assemblages that can significantly impact backscatter intensity is challenging. Consequently, it can be inferred that backscatter intensity primarily reflects substrate characteristics. On the Caiwei and Weijia seamounts, the distribution of three octocoral groups (*Chrysogorgia* spp. indet., unbranched and branched Keratoisididae), two glass sponge groups (*Farrea occa* and *Amphidiscella* spp. indet.), and Brisingida spp. indet. is predominantly influenced by backscatter intensity, exhibiting a strong preference for hard substrates. However,

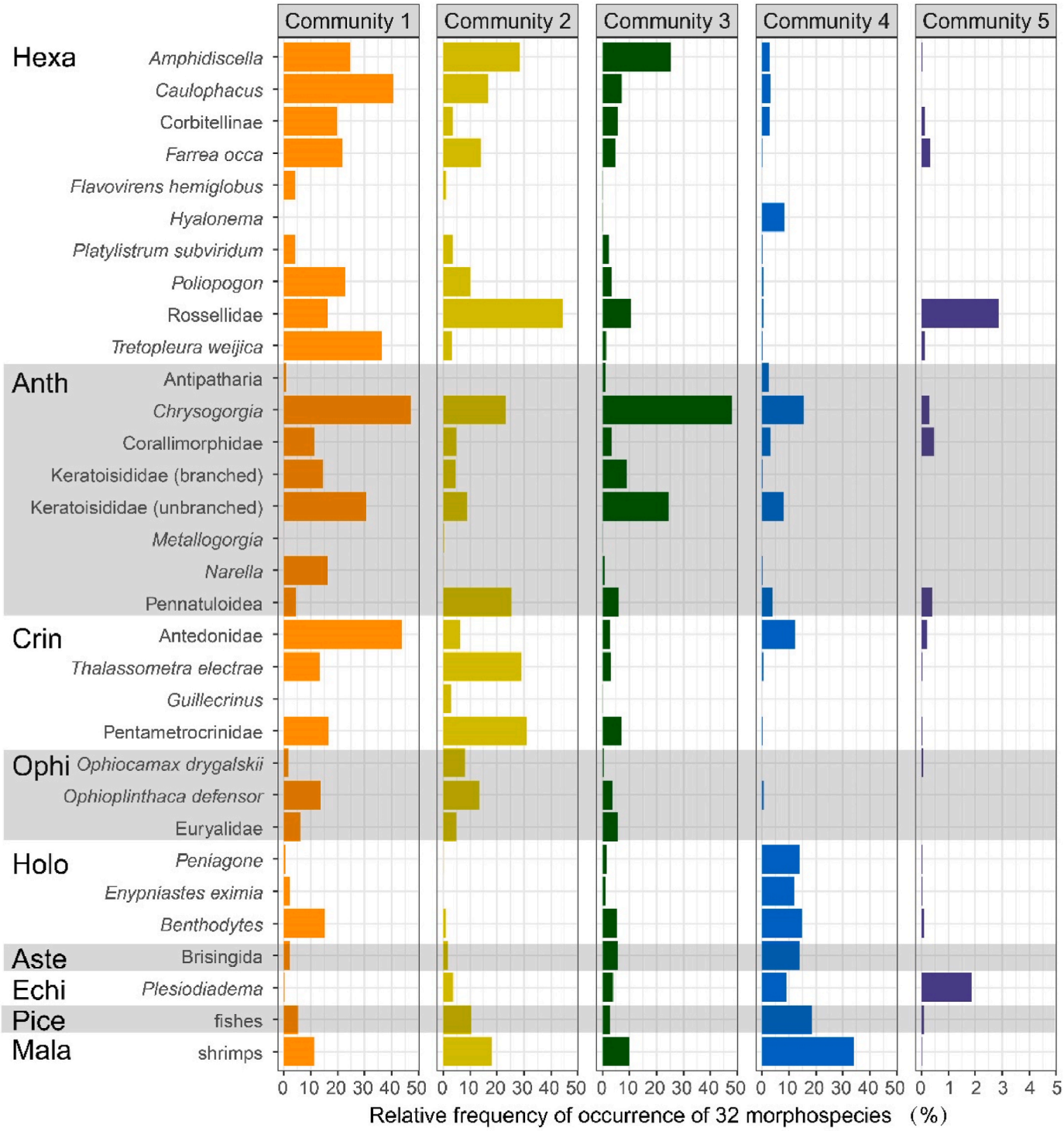

Fig. 8. Relative frequency of occurrence of 32 morphotaxa in the five communities. Hexa = class Hexactinellida; Anth = Anthozoa; Crin = class Crinoidea; Ophi = class Ophiuroidea; Holo = class Holothuroidea. Aste = class Asteroidea; Echi = class Echinoidea; Pice = superclass Pices; Mala = class Malacostraca. Morphotaxa occurring in more than 10 samples are shown.

taxa such as two glass sponge groups, *Poliopogon* spp. indet. and *Caulophacus* spp. indet., which display a greater tolerance for sediments, are less affected by backscatter intensity. In addition, the ophiuroid Euryalidae spp. indet. also showed a significant influence by backscatter intensity, due to that this group of ophiuroids is commonly associated with octocorals and sometimes stalked sponges.

4.2. Spatial heterogeneity of megabenthic communities at the single-seamount scale

Seamounts are heterogeneous habitats characterized by complexity and variability in the spatial structuring of biological communities (Clark et al., 2012). Five distinct communities were identified on the Caiwei and Weijia Seamounts in this study. Among them, Community 1 was characterized by a higher frequency of habitat-forming organisms,

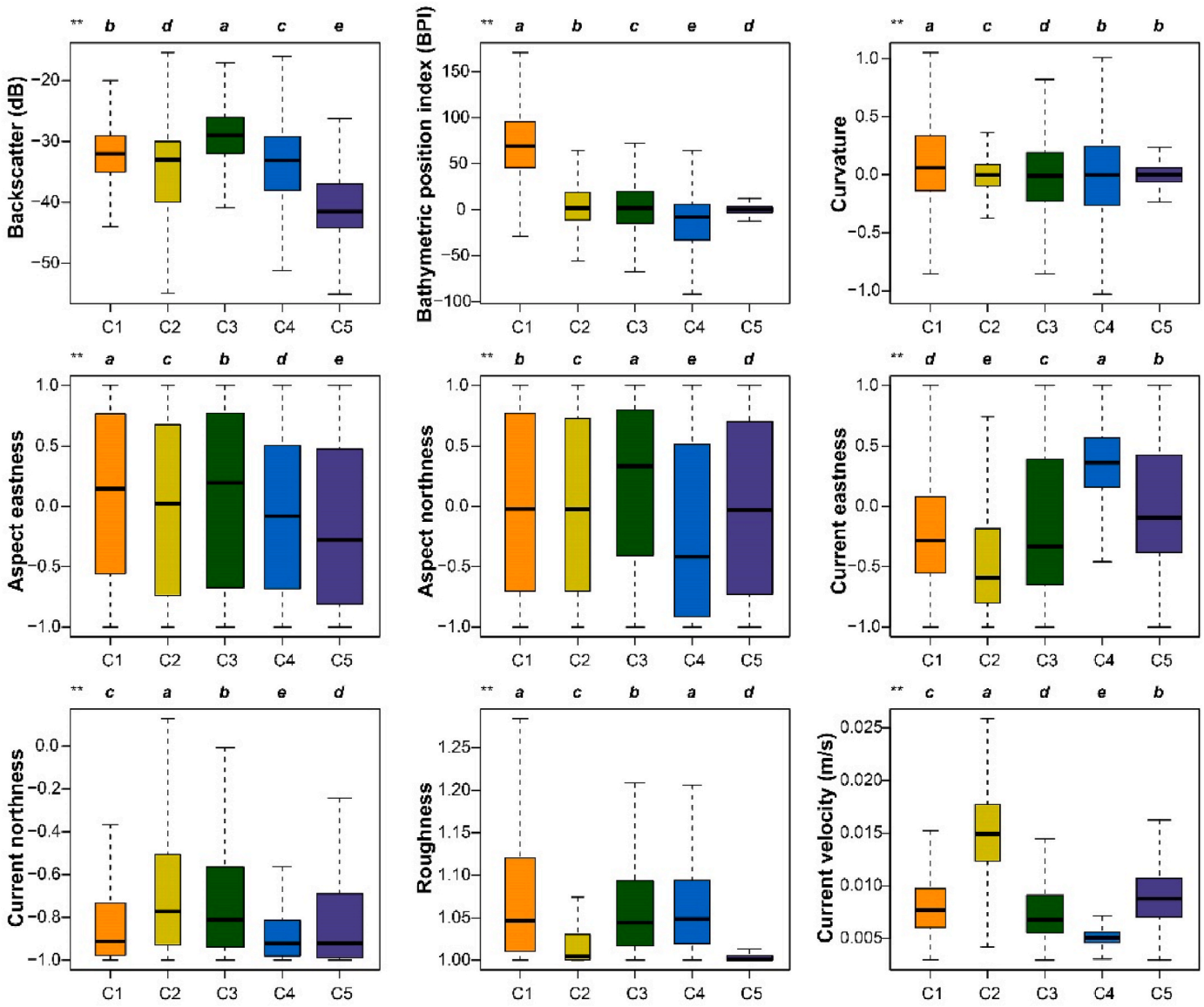

Fig. 9. Box plots of environmental variables among five communities grouped by a K-means cluster analysis. C1 to C5 refer to Community1 to Community. The Kruskal–Wallis test was used to assess the differences in environmental variables between the five communities. **refers to $P < 0.01$.

mostly including hexactinellid sponges and octocorals, which provide biogenic structures for ophiuroids and unstalked crinoids to attach and are commonly regarded as VME indicator species. Thus, Community 1 can be designated as a typical VME on deep-water seamounts. Habitat-forming organisms prefer areas with hard substrates on raised topographical features, benefiting from food enrichment by local topography-induced current flow (Shen et al., 2021b; Perez et al., 2018). Moreover, Community 2 featured a higher frequency of several kinds of crinoids, stalked sponges, and sea pens. The biological traits of crinoids occurring in Community 2 were diverse, being stalked or not stalked, solitary or associated with other organisms. The stalked crinoids are sessile and commonly identified as VME indicator species because they are fragile, slow to recover and besides, their stems can be enwound by other echinoderms, such as ophiuroids. In addition, non-sessile crinoids, which were dominant in the study area, as illustrated by Shen et al. (2021b), occurred as distinct communities in this study, implying a functional significance to deep-water seamount ecosystems. Accordingly, under the destructive disturbance caused by deep-sea mining activities, Community 2, which was dominated by diverse crinoids and several habitat-forming species, should be considered vulnerable in the study area due to its potential functional fragility. On the Caiwei and Weijia seamounts, the distribution of these two communities exhibits pronounced fragmentation, with relatively smaller areas, contributing to a higher level of vulnerability compared to the other communities (Fahrig, 2003).

Community 3 was characterized by a relatively higher frequency of several hexactinellid sponges and octocorals and an overall lower frequency of echinoderms. The occurrence of Community 3 was often adjacent to or interspersed with Communities 1 and 2. This implied that Community 3 may serve as a transitional community between Communities 1 and 2 and the other two communities. The co-occurrence of megafauna is primarily driven by similarities in environmental requirements, tolerances, and stochastic events, resulting in nondistinct community boundaries (Gleason, 1926; Keith, 2009). The occurrence of Community 3, as a transitional community, may be seen as a manifestation of these "nondistinct community boundaries". Areas of transition between homogeneous communities frequently align with pronounced environmental and ecological gradients (Kark and Van Rensburg, 2006). There is evidence to suggest that these transition zones not only uphold existing biological diversity but also serve as centers for speciation,

acting as "speciation pumps" (Goldblum and Rigg, 2010; Schilthuizen, 2000). The regions covered by these transitional communities on the Caiwei and Weijia seamounts may possess such potential. However, the relatively small scale and unremarkable species occurrence in the transition zones on the seamounts call for further investigation to ascertain this potential.

Community 4 was mainly located in the lower flanks of deep-water seamounts and featured a relatively higher frequency of diverse echinoderms, fishes and shrimps. In addition to the relatively wide occurrence of stalked sponges (belonging to the genus *Hyalonema*) preferring soft substrates, the habitats relevant to Community 4 were partially composed of soft substrates. Moreover, Community 5 exhibited extremely lower frequencies of species occurrence compared to the other communities and was distributed largely in the summits of the two deep-water seamounts. This suggested the possibility of extensive areas within the summit of deep-water seamounts devoid of megabenthic fauna. In contrast, research on shallow-water seamounts paints a different picture, emphasizing the prevalence of communities dominated by reef-building corals and sponge-dominated communities on the summits (Goode et al., 2021; Preez et al., 2016; Ramos et al., 2016). The difference arises from the fact that the Caiwei and Weijia seamounts are deep-water guyots with sediment-covered flat top platforms. The evident lower backscatter intensity and roughness indicate that the substrate on the studied summits is softer and flatter. Previous research also supported the extensive presence of pelagic sediment cover on the summit platforms of the Caiwei and Weijia seamounts (Zhao et al., 2020a, 2020b). These conditions are generally unfavorable for the survival of corals or sponges. Furthermore, a sediment study conducted on the Magellan Seamounts Chain and the Marcus-Wake Seamounts Chain revealed that the summit edges of seamounts are the areas with the lowest organic matter accumulation (Yang et al., 2020a). This is also a significant factor contributing to the scarcity of megabenthic fauna on the summits. The topographical features of flat-topped seamounts facilitate the transport of particulate organic matter from the summit down the flanks, leading to the development of an organic-rich sedimentary environment in the lower parts of the seamounts (Yang et al., 2020b). Consequently, in contrast to Community 5, which is mainly located in the summits, there is a higher frequency of occurrence of holothurians, sea urchins, fishes, and shrimps within Community 4, which is in the lower flanks of seamounts.

4.3. Similarity of community composition between the Caiwei and Weijia seamounts

There were several morphotaxa observed only on one seamount in this study, implying dissimilarity in species composition between the two seamounts. It should be noted that this feature may be caused by insufficient sampling. Total 27 dives conducted in the survey were not enough to uncover all the megabenthic fauna present on the seamounts. Species that are moderately low in abundance, or that occur in strong patches, could easily be missed. Based on the prediction of each morphotaxon in this study, the five distinct communities presented on both the Caiwei and Weijia seamounts and their distribution patterns were similar in the two seamounts, suggesting their similarity in community composition. The reliability of this result depends on the performance and uncertainty of models. The AUC values and uncertainty values confirmed the model reliability to a relatively high extent. Despite that, part of the biological data used in this study came from opportunistic sampling, which introduces sampling bias, leading to spatial differences in the uncertainty of biological prediction. The distribution results for Community 1 and Community 2 were the most trustworthy as they are situated in areas with relatively greatest sampling efforts and accordingly the lowest uncertainty. Community 3 and Community 4 were also situated in areas of lower uncertainty, though not as low as those of Community 1 and Community 2. The lower uncertainty of these communities increased the reliability of understanding on the similarity in distribution patterns of vulnerable communities between the Caiwei and Weijia seamounts. In contrast, Community 5 was widely located near the summits where model uncertainty was higher, suggesting that additional sampling may be necessary to correct potential biases. A better sampling strategy would be to first classify habitats based on environmental data and then to design survey efforts for each habitat type, thereby improving the predictive reliability (Tessarolo et al., 2014; Ferrari et al., 2018). The level of similarity or isolation of seamount populations is significantly impacted by the population connectivity between seamounts, which is a crucial factor (Clark et al., 2012). The presence of identical communities implies the potential for a high level of population connectivity across the Caiwei and Weijia seamounts (Guimarães, 2020). A previous study on the genetic population structure of species on cobalt-rich crust seamounts in the northwestern Pacific Ocean revealed that the ophiuroid species *O. defensor* on the Caiwei and Weijia seamounts belonged to a single population, providing genetic evidence on the population connectivity between the Caiwei and Weijia seamounts (Na et al., 2021). Simulation results of the hydrodynamic environment in the northwestern Pacific Ocean indicated that 20% of eddies can be advected to neighboring seamounts (Jiang et al., 2021), facilitating population exchange between these seamounts. In addition, there is another seamount situated between the Caiwei and Weijia seamounts at an approximately equal distance. According to the stepping stone hypothesis (Mazzei et al., 2021), the existence of this seamount further facilitates species dispersal between the Caiwei and Weijia seamounts.

5. Conclusions

We conducted a comprehensive mapping of benthic megafaunal distribution on two deep-water seamounts characterized by cobalt-rich crusts within the Magellan Seamount Chain in the northwestern Pacific Ocean. These species collectively constitute five distinct communities, with the average velocity and eastness of the near-bottom current, BPI, and backscatter emerging as pivotal drivers influencing the spatial distribution of these biotic assemblages. Among them, two vulnerable communities characterized by a wide occurrence of habitat-forming organisms or diverse crinoids were identified. In contrast to solely examining the distribution of VME indicator species, the broader investigation of community distribution provides a more informative perspective regarding VMEs. Moreover, the five distinct communities were distributed on the two adjacent seamounts with similar distribution patterns. This result suggested a similarity in community composition between the two deep-water seamounts and further implied potential connectivity between them. This undertaking serves as a contribution by furnishing vital descriptions of deep-water seamount communities, a crucial step in the endeavor to identify and subsequently safeguard deep-sea ecosystems.

CRediT authorship contribution statement

Runxuan Yan: Writing – original draft, Visualization, Validation, Methodology. **Chengcheng Shen:** Writing – review & editing, Supervision, Resources, Project administration, Methodology, Investigation, Funding acquisition, Formal analysis, Data curation, Conceptualization. **Dongsheng Zhang:** Writing – review & editing, Visualization, Project administration, Investigation, Formal analysis, Data curation, Conceptualization. **Zhenggang Li:** Project administration, Formal analysis, Data curation. **Leyi Fang:** Writing – review & editing, Validation. **Chunsheng Wang:** Writing – review & editing, Supervision, Investigation, Funding acquisition, Data curation.

Declaration of competing interest

The authors declare that they have no known competing financial interests or personal relationships that could have appeared to influence

the work reported in this paper.

Data availability

Data will be made available on request.

Acknowledgements

We are grateful to all the scientists and crew on the R/V "Xiangyanghong 09", "Haiyangdizhi 6" and "Dayangyihao" and the teams of HOV Jiaolong, ROV Haima and ROV Hailong III, for their dedicated research work and collection of deep-sea materials. We thank the anonymous reviewers for their constructive suggestions. This study is supported by the National Key R&D Program of China (grant number 2022YFC2806603), the National Natural Science Foundation of China (grant number 42276132), and the Scientific Research Fund of the Second Institute of Oceanography, MNR (grant number QNYC2303).

Appendix A. Supplementary data

Supplementary data to this article can be found online at https://doi.org/10.1016/j.dsr.2024.104303.

References

Anderson, O.F., Stephenson, F., Behrens, E., Rowden, A.A., 2022. Predicting the effects of climate change on deep-water coral distribution around New Zealand—will there be suitable refuges for protection at the end of the 21st century? Glob. Change Biol. 28, 6556–6576. https://doi.org/10.1111/gcb.16389.

Anderson, O.F., Guinotte, J.M., Rowden, A.A., Tracey, D.M., Mackay, K.A., Clark, M.R., 2016. Habitat suitability models for predicting the occurrence of vulnerable marine ecosystems in the seas around New Zealand. Deep Sea Res. Oceanogr. Res. Pap. 115, 265–292. https://doi.org/10.1016/j.dsr.2016.07.006.

Angelini, C., Altieri, A.H., Silliman, B.R., Bertness, M.D., 2011. Interactions among foundation species and their consequences for community organization, biodiversity, and conservation. Bioscience 61, 782–789. https://doi.org/10.1525/bio.2011.61.10.8.

Araujo, M., New, M., 2007. Ensemble forecasting of species distributions. Trends Ecol. Evol. 22, 42–47. https://doi.org/10.1016/j.tree.2006.09.010.

Ardron, J.A., Clark, M.R., Penney, A.J., Hourigan, T.F., Rowden, A.A., Dunstan, P.K., Watling, L., Shank, T.M., Tracey, D.M., Dunn, M.R., Parker, S.J., 2014. A systematic approach towards the identification and protection of vulnerable marine ecosystems. Mar. Policy 49, 146–154. https://doi.org/10.1016/j.marpol.2013.11.017.

Barbet-Massin, M., Jiguet, F., Albert, C.H., Thuiller, W., 2012. Selecting pseudo-absences for species distribution models: how, where and how many? Methods Ecol. Evol. 3, 327–338. https://doi.org/10.1111/j.2041-210X.2011.00172.x.

Bisol, P., Costa, R., Sibuet, M., 1984. Ecological and genetical survey on two deep-sea holothurians: *Benthogene rosea* and *Benthodytes typica*. Mar. Ecol. Prog. Ser. 15, 275–281. https://doi.org/10.3354/meps015275.

Bo, M., Coppari, M., Betti, F., Massa, F., Gay, G., Cattaneo-Vietti, R., Bavestrello, G., 2020. Unveiling the deep biodiversity of the Janua seamount (Ligurian sea): first Mediterranean sighting of the rare Atlantic bamboo coral *Chelidonisis aurantiaca* studer, 1890. Deep-Sea Res. Part A Oceanogr. Res. Pap. 156, 103186 https://doi.org/10.1016/j.dsr.2019.103186.

Boschen, R.E., Rowden, A.A., Clark, M.R., Gardner, J.P.A., 2013. Mining of deep-sea seafloor massive sulfides: a review of the deposits, their benthic communities, impacts from mining, regulatory frameworks and management strategies. Ocean Coast Manag. 84, 54–67. https://doi.org/10.1016/j.ocecoaman.2013.07.005.

Bridges, A.E.H., Barnes, D.K.A., Bell, J.B., Ross, R.E., Howell, K.L., 2022. Depth and latitudinal gradients of diversity in seamount benthic communities. J. Biogeogr. 49, 904–915. https://doi.org/10.1111/jbi.14355.

Bridges, A.E.H., Barnes, D.K.A., Bell, J.B., Ross, R.E., Howell, K.L., 2021. Benthic assemblage composition of south Atlantic seamounts. Front. Mar. Sci. 8, 1–18. https://doi.org/10.3389/fmars.2021.660648.

Burgos, J.M., Buhl-Mortensen, L., Buhl-Mortensen, P., Ólafsdóttir, S.H., Steingrund, P., Ragnarsson, S.Á., Skagseth, Ø., 2020. Predicting the distribution of indicator taxa of vulnerable marine ecosystems in the Arctic and sub-arctic waters of the Nordic seas. Front. Mar. Sci. 7, 1–25. https://doi.org/10.3389/fmars.2020.00131.

Clark, M.R., Althaus, F., Schlacher, T.A., Williams, A., Bowden, D.A., Rowden, A.A., 2016. The impacts of deep-sea fisheries on benthic communities: a review. ICES J. Mar. Sci. 73, i51–i69. https://doi.org/10.1093/icesjms/fsv123.

Clark, M.R., Rowden, A.A., Schlacher, T., Williams, A., Consalvey, M., Stocks, K.I., Rogers, A.D., O'Hara, T.D., White, M., Shank, T.M., Hall-Spencer, J.M., 2010. The ecology of seamounts: structure, function, and human impacts. Annu. Rev. Mar. Sci. 2, 253–278. https://doi.org/10.1146/annurev-marine-120308-081109.

Clark, M.R., Schlacher, T.A., Rowden, A.A., Stocks, K.I., Consalvey, M., 2012. Science priorities for seamounts: research links to conservation and management. PLoS One 7, e29232. https://doi.org/10.1371/journal.pone.0029232.

COMRA Office, 2018. Chinese gazetteer of undersea features on the international seabed (2017). China Ocean Press, Beijing.

De Falco, G., Tonielli, R., Di Martino, G., Innangi, S., Simeone, S., Michael Parnum, I., 2010. Relationships between multibeam backscatter, sediment grain size and *Posidonia oceanica* seagrass distribution. Continent. Shelf Res. 30, 1941–1950. https://doi.org/10.1016/j.csr.2010.09.006.

De La Torriente, A., Aguilar, R., González-Irusta, J.M., Blanco, M., Serrano, A., 2020. Habitat forming species explain taxonomic and functional diversities in a Mediterranean seamount. Ecol. Indicat. 118, 106747 https://doi.org/10.1016/j.ecolind.2020.106747.

De La Torriente, A., González-Irusta, J.M., Aguilar, R., Fernández-Salas, L.M., Punzón, A., Serrano, A., 2019. Benthic habitat modelling and mapping as a conservation tool for marine protected areas: a seamount in the western Mediterranean. Aquat. Conserv. Mar. Freshw. Ecosyst. 29, 732–750. https://doi.org/10.1002/aqc.3075.

Deka, M.A., Morshed, N., 2018. Mapping disease transmission risk of Nipah virus in South and Southeast Asia. Trav. Med. Infect. Dis. 3, 57. https://doi.org/10.3390/tropicalmed3020057.

Dijkstra, J.A., Mello, K., Sowers, D., Malik, M., Watling, L., Mayer, L.A., 2021. Fine-scale mapping of deep-sea habitat-forming species densities reveals taxonomic specific environmental drivers. Glob. Ecol. Biogeogr. 30, 1286–1298. https://doi.org/10.1111/geb.13285.

Dong, D., Xu, P., Li, X.-Z., Wang, C., 2019. *Munidopsis* species (Crustacea: Decapoda: Munidopsidae) from carcass falls in Weijia Guyot, West Pacific, with recognition of a new species based on integrative taxonomy. PeerJ 7, e8089. https://doi.org/10.7717/peerj.8089.

Dormann, C.F., Elith, J., Bacher, S., Buchmann, C., Carl, G., Carré, G., Marquéz, J.R.G., Gruber, B., Lafourcade, B., Leitão, P.J., Münkemüller, T., McClean, C., Osborne, P.E., Reineking, B., Schröder, B., Skidmore, A.K., Zurell, D., Lautenbach, S., 2013. Collinearity: a review of methods to deal with it and a simulation study evaluating their performance. Ecography 36, 27–46. https://doi.org/10.1111/j.1600-0587.2012.07348.x.

Du, D., Ren, X., Yan, S., Shi, X., Liu, Y., He, G., 2017. An integrated method for the quantitative evaluation of mineral resources of cobalt-rich crusts on seamounts. Ore Geol. Rev. 84, 174–184. https://doi.org/10.1016/j.oregeorev.2017.01.011.

Fahrig, L., 2003. Effects of habitat fragmentation on biodiversity. Annu. Rev. Ecol. Evol. Syst. 34, 487–515. https://doi.org/10.1146/annurev.ecolsys.34.011802.132419.

Fan, M., Shi, S., Ma, Y., Wang, H., Zhai, J., Zhang, X., Ning, P., 2022. High resolution geomorphological classification of benthic structure on the Western Pacific Seamount. Front. Mar. Sci. 9, 1–17. https://doi.org/10.3389/fmars.2022.1007032.

Ferrari, R., Malcolm, H., Neilson, J., Lucieer, V., Jordan, A., Ingleton, T., Figueira, W., Johnstone, N., Hill, N., 2018. Integrating distribution models and habitat classification maps into marine protected area planning. Estuar. Coast Shelf Sci. 212, 40–50. https://doi.org/10.1016/j.ecss.2018.06.015.

Gama, M., Crespo, D., Dolbeth, M., Anastácio, P.M., 2017. Ensemble forecasting of *Corbicula fluminea* worldwide distribution: Projections of the impact of climate change. Aquat. Conserv. Mar. Freshw. Ecosyst. 27, 675–684. https://doi.org/10.1002/aqc.2767.

Georgian, S.E., Anderson, O.F., Rowden, A.A., 2019. Ensemble habitat suitability modeling of vulnerable marine ecosystem indicator taxa to inform deep-sea fisheries management in the South Pacific Ocean. Fish. Res. 211, 256–274. https://doi.org/10.1016/j.fishres.2018.11.020.

Gleason, H.A., 1926. The individualistic concept of the plant association. Bull. Torrey Bot. Club 53, 7–26. https://doi.org/10.2307/2479933.

Glover, A.G., Smith, C.R., 2003. The deep-sea floor ecosystem: current status and prospects of anthropogenic change by the year 2025. Environ. Conserv. 30, 219–241. https://doi.org/10.1017/S0376892903000225.

Goldblum, D., Rigg, L.S., 2010. The deciduous forest – boreal forest ecotone. Geogr. Compass 4, 701–717. https://doi.org/10.1111/j.1749-8198.2010.00342.x.

Gollner, S., Kaiser, S., Menzel, L., Jones, D.O.B., Brown, A., Mestre, N.C., van Oevelen, D., Menot, L., Colaço, A., Canals, M., Cuvelier, D., Durden, J.M., Gebruk, A., Egho, G.A., Haeckel, M., Marcon, Y., Mevenkamp, L., Morato, T., Pham, C.K., Purser, A., Sanchez-Vidal, A., Vanreusel, A., Vink, A., Martinez Arbizu, P., 2017. Resilience of benthic deep-sea fauna to mining activities. Mar. Environ. Res. 129, 76–101. https://doi.org/10.1016/j.marenvres.2017.04.010.

González-Irusta, J.M., González-Porto, M., Sarralde, R., Arrese, B., Almón, B., Martín-Sosa, P., 2015. Comparing species distribution models: a case study of four deep sea urchin species. Hydrobiologia 745, 43–57. https://doi.org/10.1007/s10750-014-2090-3.

Gonzalez-Mirelis, G., 2021. Modeling the distribution of habitat-forming, Deep-Sea sponges in the Barents sea: the value of data. Front. Mar. Sci. 7, 1–14. https://doi.org/10.3389/fmars.2020.496688.

Goode, S.L., Rowden, A.A., Bowden, D.A., Clark, M.R., Stephenson, F., 2021. Fine-scale mapping of Mega-Epibenthic communities and their Patch characteristics on two New Zealand seamounts. Front. Mar. Sci. 8, 1–21. https://doi.org/10.3389/fmars.2021.765407.

Graves, K.P., Bridges, A.E.H., Dabrowski, T., Furey, T., Lyons, K., Howell, K.L., 2023. Oceanographic variability drives the distribution but not the density of the aggregation forming deep-sea sponge *Pheronema carpenteri*. Deep-Sea Res. Part A Oceanogr. Res. Pap. 191, 103917 https://doi.org/10.1016/j.dsr.2022.103917.

Guimarães, P.R., 2020. The structure of ecological networks across levels of organization. Annu. Rev. Ecol. Evol. Syst. 51, 433–460. https://doi.org/10.1146/annurev-ecolsys-012220-120819.

Hamilton, W.B., 2003. An alternative earth. GSA Today (Geol. Soc. Am.) 13, 4. https://doi.org/10.1130/1052-5173(2003)013<0004:AAE>2.0.CO;2.

Handley, S.J., Willis, T.J., Cole, R.G., Bradley, A., Cairney, D.J., Brown, S.N., Carter, M. E., 2014. The importance of benchmarking habitat structure and composition for

understanding the extent of fishing impacts in soft sediment ecosystems. J. Sea Res. 86, 58–68. https://doi.org/10.1016/j.seares.2013.11.005.
Hefley, T.J., Tyre, A.J., Baasch, D.M., Blankenship, E.E., 2013. Nondetection sampling bias in marked presence-only data. Ecol. Evol. 3, 5225–5236. https://doi.org/10.1002/ece3.887.
Henson, S.A., Sanders, R., Madsen, E., 2012. Global patterns in efficiency of particulate organic carbon export and transfer to the deep ocean. Glob. Biogeochem. Cycles 26. https://doi.org/10.1029/2011GB004099.
Holmes, K.W., Van Niel, K.P., Radford, B., Kendrick, G.A., Grove, S.L., 2008. Modelling distribution of marine benthos from hydroacoustics and underwater video. Continent. Shelf Res. 28, 1800–1810. https://doi.org/10.1016/j.csr.2008.04.016.
Jiang, X., Dong, C., Ji, Y., Wang, C., Shu, Y., Liu, L., Ji, J., 2021. Influences of deep-water seamounts on the hydrodynamic environment in the northwestern Pacific Ocean. J. Geophys. Res. Oceans 126, e2021JC017396. https://doi.org/10.1029/2021JC017396.
Jones, D.O.B., Amon, D.J., Chapman, A.S.A., 2018. Mining deep-ocean mineral deposits: what are the ecological risks? Elements 14, 325–330. https://doi.org/10.2138/gselements.14.5.325.
Kark, S., Van Rensburg, B.J., 2006. Ecotones: marginal or central areas of transition? Isr. J. Ecol. Evol. 52, 29–53. https://doi.org/10.1560/IJEE.52.1.29.
Kearney, M., Porter, W., 2009. Mechanistic niche modelling: combining physiological and spatial data to predict species' ranges. Ecol. Lett. 12, 334–350. https://doi.org/10.1111/j.1461-0248.2008.01277.x.
Keith, D.A., 2009. The interpretation, assessment and conservation of ecological communities. Ecol. Manag. Restor. 10 https://doi.org/10.1111/j.1442-8903.2009.00453.x.
Kremenetskaia, A., Gebruk, A., Alt, C.H.S., Budaeva, N., 2021. New and poorly known species of *Peniagone* (Holothuroidea, Elpidiidae) from the northwest Pacific Ocean with discussion on Phylogeny of the genus. Diversity 13, 541. https://doi.org/10.3390/d13110541.
Kvile, K.Ø., Taranto, G.H., Pitcher, T.J., Morato, T., 2014. A global assessment of seamount ecosystems knowledge using an ecosystem evaluation framework. Biol. Conserv. 173, 108–120. https://doi.org/10.1016/j.biocon.2013.10.002.
Leduc, D., Rowden, A.A., Nodder, S.D., Berkenbusch, K., Probert, P.K., Hadfield, M.G., 2014. Unusually high food availability in Kaikoura Canyon linked to distinct deep-sea nematode community. Deep Sea Res. Part II Top. Stud. Oceanogr., Submarine Canyons: Complex Deep-Sea Environments Unravelled by Multidisciplinary Research 104, 310–318. https://doi.org/10.1016/j.dsr2.2013.06.003.
Leitner, A.B., Drazen, J.C., Smith, C.R., 2021. Testing the seamount refuge hypothesis for predators and scavengers in the western Clarion-Clipperton zone. Front. Mar. Sci. 8, 636305 https://doi.org/10.3389/fmars.2021.636305.
Li, Z., Li, H., Hein, J.R., Dong, Y., Wang, M., Ren, X., Wu, Z., Li, X., Chu, F., 2021. A possible link between seamount sector collapse and manganese nodule occurrence in the abyssal plains, NW Pacific Ocean. Ore Geol. Rev. 138, 104378 https://doi.org/10.1016/j.oregeorev.2021.104378.
Mazzei, E.F., Pinheiro, H.T., Simon, T., Moura, R.L., Macieira, R.M., Pimentel, C.R., Teixeira, J.B., Floeter, S.R., Ferreira, C.E.L., Ghisolfi, R.D., Francini-Filho, R.B., Quimbayo, J.P., Rocha, L.A., Gasparini, J.L., Joyeux, J.-C., 2021. Mechanisms of dispersal and establishment drive a stepping stone community assembly on seamounts and oceanic islands. Mar. Biol. 168, 109. https://doi.org/10.1007/s00227-021-03919-7.
Mestre, N.C., Rocha, T.L., Canals, M., Cardoso, C., Danovaro, R., Dell'Anno, A., Gambi, C., Regoli, F., Sanchez-Vidal, A., Bebianno, M.J., 2017. Environmental hazard assessment of a marine mine tailings deposit site and potential implications for deep-sea mining. Environ. Pollut. 228, 169–178. https://doi.org/10.1016/j.envpol.2017.05.027.
Miller, K.A., Thompson, K.F., Johnston, P., Santillo, D., 2018. An overview of seabed mining including the current state of development, environmental impacts, and knowledge Gaps. Front. Mar. Sci. 4, 1–24. https://doi.org/10.3389/fmars.2017.00418.
Miyamoto, M., Kiyota, M., Murase, H., Nakamura, T., Hayashibara, T., 2017. Effects of bathymetric grid-cell sizes on habitat suitability analysis of cold-water Gorgonian corals on seamounts. Mar. Geod. 40, 205–223. https://doi.org/10.1080/01490419.2017.1315543.
Morel, A., Claustre, H., Gentili, B., 2010. The most oligotrophic subtropical zones of the global ocean: similarities and differences in terms of chlorophyll and yellow substance. Biogeosciences 7, 3139–3151. https://doi.org/10.5194/bg-7-3139-2010.
Morgan, N.B., Cairns, S., Reiswig, H., Baco, A.R., 2015. Benthic megafaunal community structure of cobalt-rich manganese crusts on Necker Ridge. Deep-Sea Res. Part A Oceanogr. Res. Pap. 104, 92–105. https://doi.org/10.1016/j.dsr.2015.07.003.
Muñoz-Royo, C., Peacock, T., Alford, M.H., Smith, J.A., Le Boyer, A., Kulkarni, C.S., Lermusiaux, P.F.J., Haley, P.J., Mirabito, C., Wang, D., Adams, E.E., Ouillon, R., Breugem, A., Decrop, B., Lanckriet, T., Supekar, R.B., Rzeznik, A.J., Gartman, A., Ju, S.-J., 2021. Extent of impact of deep-sea nodule mining midwater plumes is influenced by sediment loading, turbulence and thresholds. Commun. Earth Environ. 2, 1–16. https://doi.org/10.1038/s43247-021-00213-8.
Na, J., Chen, W., Zhang, D., Zhang, R., Lu, B., Shen, C., Zhou, Y., Wang, C., 2021. Morphological description and population structure of an ophiuroid species from cobalt-rich crust seamounts in the Northwest Pacific: implications for marine protection under deep-sea mining. Acta Oceanol. Sin. 40, 79–89. https://doi.org/10.1007/s13131-020-1666-1.
Naimi, B., Hamm, N.A.S., Groen, T.A., Skidmore, A.K., Toxopeus, A.G., 2014. Where is positional uncertainty a problem for species distribution modelling? Ecography 37, 191–203. https://doi.org/10.1111/j.1600-0587.2013.00205.x.
O'Hara, T.D., Consalvey, M., Lavrado, H.P., Stocks, K.I., 2010. Environmental predictors and turnover of biota along a seamount chain: assemblage composition along a seamount chain. Mar. Ecol. 31, 84–94. https://doi.org/10.1111/j.1439-0485.2010.00379.x.
O'Neill, F.G., Robertson, M., Summerbell, K., Breen, M., Robinson, L.A., 2013. The mobilisation of sediment and benthic infauna by scallop dredges. Mar. Environ. Res. 90, 104–112. https://doi.org/10.1016/j.marenvres.2013.06.003.
Perez, J.A.A., Kitazato, H., Sumida, P.Y.G., Sant'Ana, R., Mastella, A.M., 2018. Benthopelagic megafauna assemblages of the Rio Grande rise (SW Atlantic). Deep-Sea Res. Part A Oceanogr. Res. Pap. 134, 1–11. https://doi.org/10.1016/j.dsr.2018.03.001.
Pinheiro, M., Oliveira, A., Barros, S., Alves, N., Raimundo, J., Caetano, M., Coimbra, J., Neuparth, T., Santos, M.M., 2021. Functional, biochemical and molecular impact of sediment plumes from deep-sea mining on *Mytilus galloprovincialis* under hyperbaric conditions. Environ. Res. 195, 110753 https://doi.org/10.1016/j.envres.2021.110753.
Preez, C.D., Curtis, J.M.R., Clarke, M.E., 2016. The structure and distribution of benthic communities on a shallow seamount (Cobb seamount, Northeast Pacific Ocean). PLoS One 11, e0165513. https://doi.org/10.1371/journal.pone.0165513.
Ramiro-Sánchez, B., González-Irusta, J.M., Henry, L.-A., Cleland, J., Yeo, I., Xavier, J.R., Carreiro-Silva, M., Sampaio, Í., Spearman, J., Victorero, L., Messing, C.G., Kazanidis, G., Roberts, J.M., Murton, B., 2019. Characterization and mapping of a deep-sea sponge ground on the Tropic seamount (Northeast tropical Atlantic): implications for spatial management in the high seas. Front. Mar. Sci. 6 https://doi.org/10.3389/fmars.2019.00278.
Ramos, M., Bertocci, I., Tempera, F., Calado, G., Albuquerque, M., Duarte, P., 2016. Patterns in megabenthic assemblages on a seamount summit (Ormonde Peak, Gorringe bank, Northeast Atlantic). Mar. Ecol. 37, 1057–1072. https://doi.org/10.1111/maec.12353.
Robert, K., Jones, D.O.B., Roberts, J.M., Huvenne, V.A.I., 2016. Improving predictive mapping of deep-water habitats: considering multiple model outputs and ensemble techniques. Deep-Sea Res. Part A Oceanogr. Res. Pap. 113, 80–89. https://doi.org/10.1016/j.dsr.2016.04.008.
Robison, B.H., 1992. Bioluminescence in the benthopelagic holothurian *Enypniastes eximia*. J. Mar. Biol. Assoc. U. K. 72, 463–472. https://doi.org/10.1017/S0025315400037826.
Rodríguez-Basalo, A., Prado, E., Sánchez, F., Ríos, P., Gómez-Ballesteros, M., Cristobo, J., 2021. High resolution spatial distribution for the hexactinellid sponges *Asconema setubalense* and *Pheronema carpenteri* in the central Cantabrian sea. Front. Mar. Sci. 8, 1–15. https://doi.org/10.3389/fmars.2021.612761.
Ross, S.W., Rhode, M., Quattrini, A.M., 2015. Demersal fish distribution and habitat use within and near Baltimore and Norfolk Canyons, U.S. middle Atlantic slope. Deep-Sea Res. Part A Oceanogr. Res. Pap. 103, 137–154. https://doi.org/10.1016/j.dsr.2015.06.004.
Schilthuizen, M., 2000. Ecotone: speciation-prone. Trends Ecol. Evol. 15, 130–131. https://doi.org/10.1016/S0169-5347(00)01839-5.
Schlacher, T.A., Baco, A.R., Rowden, A.A., O'Hara, T.D., Clark, M.R., Kelley, C., Dower, J.F., 2014. Seamount benthos in a cobalt-rich crust region of the central Pacific: conservation challenges for future seabed mining. Divers. Distrib. 20, 491–502. https://doi.org/10.1111/ddi.12142.
Schlacher, T.A., Rowden, A.A., Dower, J.F., Consalvey, M., 2010. Seamount science scales undersea mountains: new research and outlook. Mar. Ecol. 31, 1–13. https://doi.org/10.1111/j.1439-0485.2010.00396.x.
Shen, C., Cheng, H., Zhang, D., Lu, B., Wang, C., 2021a. A new species of the glass sponge genus *Walteria* (Hexactinellida: Lyssacinosida: Euplectellidae) from northwestern Pacific seamounts, providing a biogenic microhabitat in the deep sea. Acta Oceanol. Sin. 40, 39–49. https://doi.org/10.1007/s13131-021-1939-3.
Shen, C., Lu, B., Li, Z., Zhang, R., Chen, W., Xu, P., Yao, H., Chen, Z., Pang, J., Wang, C., Zhang, D., 2021b. Community structure of benthic megafauna on a seamount with cobalt-rich ferromanganese crusts in the northwestern Pacific Ocean. Deep-Sea Res. Part A Oceanogr. Res. Pap. 178, 103661 https://doi.org/10.1016/j.dsr.2021.103661.
Swanborn, D.J.B., Huvenne, V.A.I., Pittman, S.J., Rogers, A.D., Taylor, M.L., Woodall, L. C., 2023. Mapping, quantifying and comparing seascape heterogeneity of Southwest Indian Ridge seamounts. Landsc. Ecol. 38, 185–203. https://doi.org/10.1007/s10980-022-01541-6.
Tapia-Guerra, J.M., Mecho, A., Easton, E.E., Gallardo, M. de los Á., Gorny, M., Sellanes, J., 2021. First description of deep benthic habitats and communities of oceanic islands and seamounts of the Nazca Desventuradas Marine Park, Chile. Sci. Rep. 11, 6209. https://doi.org/10.1038/s41598-021-85516-8.
Taranto, G.H., González-Irusta, J.-M., Dominguez-Carrió, C., Pham, C.K., Tempera, F., Ramos, M., Gonçalves, G., Carreiro-Silva, M., Morato, T., 2023. Spatial distributions, environmental drivers and co-existence patterns of key cold-water corals in the deep sea of the Azores (NE Atlantic). Deep-Sea Res. Part A Oceanogr. Res. Pap. 197, 104028 https://doi.org/10.1016/j.dsr.2023.104028.
Tessarolo, G., Rangel, T.F., Araújo, M.B., Hortal, J., 2014. Uncertainty associated with survey design in species distribution models. Divers. Distrib. 20, 1258–1269. https://doi.org/10.1111/ddi.12236.
Tunnicliffe, V., Metaxas, A., Le, J., Ramirez-Llodra, E., Levin, L.A., 2020. Strategic environmental goals and objectives: setting the basis for environmental regulation of deep seabed mining. Mar. Policy, Environmental governance of deep seabed mining - scientific insights and food for thought 114, 103347. https://doi.org/10.1016/j.marpol.2018.11.010.
Uhlenkott, K., Simon-Lledó, E., Vink, A., Martínez Arbizu, P., 2022. Investigating the benthic megafauna in the eastern Clarion Clipperton Fracture Zone (north-east Pacific) based on distribution models predicted with random forest. Sci. Rep. 12, 8229. https://doi.org/10.1038/s41598-022-12323-0.

Van Der Grient, J.M.A., Drazen, J.C., 2021. Potential spatial intersection between high-seas fisheries and deep-sea mining in international waters. Mar. Policy 129, 104564. https://doi.org/10.1016/j.marpol.2021.104564.

van Denderen, P.D., Holah, H., Robson, L.M., Hiddink, J.G., Menot, L., Pedreschi, D., Kazanidis, G., Llope, M., Turner, P.J., Stirling, D., Murillo, F.J., Kenny, A., Campbell, N., Allcock, A.L., Braga-Henriques, A., González-Irusta, J.M., Johnston, G., Orejas, C., Serrano, A., Xavier, J.R., Hopkins, P., Kenchington, E., Nixon, E., Valanko, S., 2022. A policy-based framework for the determination of management options to protect vulnerable marine ecosystems under the EU deep-sea access regulations. ICES J. Mar. Sci. 79, 34–49. https://doi.org/10.1093/icesjms/fsab237.

Victorero, L., Robert, K., Robinson, L.F., Taylor, M.L., Huvenne, V.A.I., 2018. Species replacement dominates megabenthos beta diversity in a remote seamount setting. Sci. Rep. 8, 4152. https://doi.org/10.1038/s41598-018-22296-8.

Vierod, A.D.T., Guinotte, J.M., Davies, A.J., 2014. Predicting the distribution of vulnerable marine ecosystems in the deep sea using presence-background models. Deep Sea Res. Part II Top. Stud. Oceanogr. 99, 6–18. https://doi.org/10.1016/j.dsr2.2013.06.010.

Watling, L., Auster, P.J., 2021. Vulnerable marine ecosystems, communities, and indicator species: confusing concepts for conservation of seamounts. Front. Mar. Sci. 8, 1–7. https://doi.org/10.3389/fmars.2021.622586.

Watling, L., Auster, P.J., 2017. Seamounts on the high seas should be managed as vulnerable marine ecosystems. Front. Mar. Sci. 4, 1–4. https://doi.org/10.3389/fmars.2017.00014.

Wilson, M.F.J., O'Connell, B., Brown, C., Guinan, J.C., Grehan, A.J., 2007. Multiscale terrain analysis of multibeam bathymetry data for habitat mapping on the continental slope. Mar. Geod. 30, 3–35. https://doi.org/10.1080/01490410701295962.

Xu, K., 2021. Exploring seamount ecosystems and biodiversity in the tropical Western Pacific Ocean. J. Oceanol. Limnol. 39, 1585–1590. https://doi.org/10.1007/s00343-021-1585-9.

Xu, P., Zhou, Y., Wang, C., 2017. A new species of deep-sea sponge-associated shrimp from the North-West Pacific (Decapoda, Stenopodidea, Spongicolidae). ZooKeys 1–14. https://doi.org/10.3897/zookeys.685.11341.

Yang, Y., He, G., Ma, J., Yu, Z., Yao, H., Deng, X., Liu, F., Wei, Z., 2020a. Acoustic quantitative analysis of ferromanganese nodules and cobalt-rich crusts distribution areas using EM122 multibeam backscatter data from deep-sea basin to seamount in Western Pacific Ocean. Deep-Sea Res. Part A Oceanogr. Res. Pap. 161, 103281 https://doi.org/10.1016/j.dsr.2020.103281.

Yang, Z., Qian, Q., Chen, M., Zhang, R., Yang, W., Zheng, M., Qiu, Y., 2020b. Enhanced but highly variable bioturbation around seamounts in the northwest Pacific. Deep-Sea Res. Part A Oceanogr. Res. Pap. 156, 103190 https://doi.org/10.1016/j.dsr.2019.103190.

Yesson, C., Clark, M.R., Taylor, M.L., Rogers, A.D., 2011. The global distribution of seamounts based on 30 arc seconds bathymetry data. Deep-Sea Res. Part A Oceanogr. Res. Pap. 58, 442–453. https://doi.org/10.1016/j.dsr.2011.02.004.

Zhao, B., Wei, Z., Yang, Y., He, G., Zhang, H., Ma, W., 2020a. Sedimentary characteristics and the implications of cobalt-rich crusts resources at Caiwei guyot in the western Pacific Ocean. Mar. Georesources Geotechnol. 38, 1037–1045. https://doi.org/10.1080/1064119X.2019.1648615.

Zhao, B., Yang, Y., Zhang, X., He, G., Lü, W., Liu, Y., Wei, Z., Deng, Y., Huang, N., 2020b. Sedimentary characteristics based on sub-bottom profiling and the implications for mineralization of cobalt-rich ferromanganese crusts at Weijia Guyot, Western Pacific Ocean. Deep-Sea Res. Part A Oceanogr. Res. Pap. 158, 103223 https://doi.org/10.1016/j.dsr.2020.103223.

Zhao, G., Cui, X., Sun, J., Li, T., Wang, Q., Ye, X., Fan, B., 2021. Analysis of the distribution pattern of Chinese Ziziphus jujuba under climate change based on optimized biomod2 and MaxEnt models. Ecol. Indicat. 132, 108256 https://doi.org/10.1016/j.ecolind.2021.108256.